

EMERGENT LEADER CELLS IN COLLECTIVE CELL MIGRATION IN
IN VITRO WOUND HEALING ASSAY

By

Yongliang Yang

A Dissertation Submitted to the Faculty of the
DEPARTMENT OF AEROSPACE AND MECHANICAL ENGINEERING

In Partial Fulfillment of the Requirements

For the Degree of

DOCTOR OF PHILOSOPHY

WITH A MAJOR IN MECHANICAL ENGINEERING

In the Graduate College

THE UNIVERSITY OF ARIZONA

2014

THE UNIVERSITY OF ARIZONA
GRADUATE COLLEGE

As members of the Dissertation Committee, we certify that we have read the dissertation prepared by Yongliang Yang, titled *Emergent Leader Cells in Collective Cell Migration in In Vitro Wound Healing Assay* and recommend that it be accepted as fulfilling the dissertation requirement for the Degree of Doctor of Philosophy.

Date: (07/16/2014)

Pak Kin Wong

Date: (07/16/2014)

Yishak Zohar

Date: (07/16/2014)

Xiaoyi Wu

Date: (07/16/2014)

Peiwen Li

Final approval and acceptance of this dissertation is contingent upon the candidate's submission of the final copies of the dissertation to the Graduate College. I hereby certify that I have read this dissertation prepared under my direction and recommend that it be accepted as fulfilling the dissertation requirement.

Date: (08/12/2014)

Dissertation Director: Pak Kin Wong

STATEMENT BY AUTHOR

This dissertation has been submitted in partial fulfillment of the requirements for an advanced degree at the University of Arizona and is deposited in the University Library to be made available to borrowers under rules of the Library.

Brief quotations from this dissertation are allowable without special permission, provided that an accurate acknowledgement of the source is made. Requests for permission for extended quotation from or reproduction of this manuscript in whole or in part may be granted by the head of the major department or the Dean of the Graduate College when in his or her judgment the proposed use of the material is in the interests of scholarship. In all other instances, however, permission must be obtained from the author.

SIGNED: Yongliang Yang

ACKNOWLEDGEMENTS

First and foremost I would like to appreciate my advisor, Dr Pak Kin Wong. His open mind and rigor on research have been printed in my mind to guide my career in the future. Though tough Dr Wong's requirement on science is, I really appreciate his encouragement and support when I experienced difficulties during my research in the past five years. This combination of rigor and kindness is the most important thing I have learnt from Dr Wong. I thank my committee members, Dr Zohar, Dr Wu, and Dr Li. All of them helped me dedicatedly on my research and career issues in the past five years.

I am indebted to Dr Wen J. Li, my advisor when I was in Shenyang, for his support and encouragement. Without those, I cannot imagine I can pursue my PhD in this country.

I also want to thank my all lab mates in systematic bioengineering laboratory. Without their help, I can finish nothing here. I would like to thank Dr Zhang and her students for their support in my research.

DEDICATION

To

L, W and my family

TABLE OF CONTENTS

| | |
|--|----|
| LIST OF FIGURES | 10 |
| NOMENCLATURE | 19 |
| ABSTRACT | 20 |
| CHAPTER 1 INTRODUCTION | 22 |
| 1.1 Collective cell migration | 22 |
| 1.2 <i>In Vitro</i> wound healing assay, and emergent leader cells | 26 |
| 1.3 Arsenic, collective cell migration, and Nrf2 signaling pathway | 31 |
| 1.4 Main hypothesis and structure of this research | 33 |
| 1.5 Specific aims..... | 37 |
| CHAPTER 2 BACKGROUND | 39 |
| 2.1 Wounding methods..... | 40 |
| 2.2 Observation method in wound healing assay..... | 48 |
| 2.3 Summary..... | 51 |

| | |
|--|----|
| CHAPTER 3 METHODS | 52 |
| 3.1 Cell culture..... | 52 |
| 3.2 <i>In Vitro</i> wound healing assay..... | 53 |
| 3.3 Plasma lithography enhanced wound healing assay..... | 54 |
| 3.4 Immunofluorescence staining..... | 57 |
| 3.5 PIV analysis and post-analysis data processing..... | 59 |
| 3.6 siRNA gene silencing..... | 62 |
| 3.7 Western blot assay..... | 63 |
| CHAPTER 4 EMERGENT LEADER CELLS GUIDE ENDOTHELIAL CELL MONOLAYER MIGRATION IN <i>IN VITRO</i> WOUND HEALING ASSAY | |
| | 66 |
| 4.1 Introduction and objective..... | 66 |
| 4.2 Injury level do not affect the cell monolayer migration rates | 68 |

| | |
|---|-----|
| 4.3 Leader cell density and cell monolayer migration rates are robust relatively to the width of the rectangular cell monolayer | 70 |
| 4.4 Leader cells guide the cell monolayer migrating towards the cell-free region..... | 76 |
| 4.5 Regulating leader cell density and cell monolayer migration rates via changing geometry of cell monolayer in in vitro wound healing assay | 86 |
| 4.6 Higher leader cell density enhances the correlation level of the cell migration during collective cell migration | 92 |
| 4.7 Discussion | 100 |
| CHAPTER 5 ARSENIC TREATMENT ENHANCES KERATINOCYTE | |
| MONOLAYER LEADER CELL FORMATION AND MIGRATION DYNAMICS | |
| | 108 |
| 5.1 Introduction and objective..... | 108 |
| 5.2 Arsenic affects collective cell migration rate with a dose dependent manner | 111 |

| | |
|---|-----|
| 5.3 Proliferation induced by arsenic do not contribute on its effects on collective cell migration..... | 117 |
| 5.4 Arsenic affects the phenotype of the emergent leader cells..... | 120 |
| 5.5 Arsenic modulates actin stress fiber and focal adhesion sites..... | 122 |
| 5.6 Arsenic modulates E-cadherin to change the cell correlation level..... | 125 |
| 5.7 Nrf2 signaling pathway involves arsenic enhanced cell monolayer migration... | 126 |
| 5.8 Nrf2 signaling pathway affects the cell migration rates and correlation level | 131 |
| CHAPTER 6 CONCLUSION..... | 134 |
| REFERENCES..... | 136 |

LIST OF FIGURES

| | |
|---|----|
| Figure 1 Plasma lithography enhanced <i>in vitro</i> wound healing assay. (A) Plasma lithography to generate the selectively functionalized substrate; (B) cell seeding; After placed the DPMS blockers, cells are seeded into the petri dish; (C) Wounding and observing the healing process. After the cell monolayer is formed, the PDMS blockers are removed and cell migration is recorded. | 55 |
| Figure 2 The concept of the correlation level. The correlation level between the wound leading edge with 100 μm deep and the area of R μm distance and ΔR deep. For each unit in the frontier, the correlation between it and each units in the following area was calculated. Then the final correlation level for distance R is the average correlation value of all units in the frontier. | 61 |
| Figure 3 Injury level do not affect the cell monolayer migration rates in geometrical confined cell monolayer and without confinement. | 69 |
| Figure 4. The cell monolayer migration rates are constant within first 10 hours after wounding. (A) Representative images of plasma lithography enhanced wound healing | |

assay; (B) The relationship of displacement of the wounding leading edge and time after wounding.72

Figure 5. The cell monolayer migration rates and the number of leader cells are constant with various widths of the rectangular patterns. (A) Cell monolayer migration rates under various widths of rectangular cell monolayer migration; (B) The leader cell number is linear proportional to the width of the rectangular cell monolayer. The dashed line representative to the 95% confidential interval.73

Figure 6. Representative images of the leader cells in rectangular cell monolayer patterns with various widths. Scale bar 50 μm74

Figure 7. The size and length of frontier cells are significantly different from the cells in the inner region of the cell monolayer75

Figure 8. The free perimeter of leader cells is around two folds larger than that of the other cells at the leading edge79

Figure 9. The migration rates at the wound leading edge are unevenly distributed. The distance between the two fast migrating cell groups is in the same level of the distance between two nearby leader cells80

Figure 10. The leader cells maintains a high distribution frequency at the boundary of the rectangular pattern, and the cells at boundary migrates significantly faster than the cells at the center of the cell monolayer. (A) Representative images of the leader cell location; (B) the distribution frequency of the leader cells along the leading edge; (C) the migration rates of the boundary and center region of the leading edge.81

Figure 11. The actin stress fiber in the follower cells are aligned towards their leader cells, and the frontier cells and leader cells have a higher expression level of stress fiber compared with the cells in the inner region of the monolayer. (A) Actin stress fiber distribution within cells in wound healing assay; (B) the stress fiber of leader cells; (C) the alignment of the stress fiber of follower cells to their leader cells; (D) the stress fiber expression in the inner region of monolayer82

Figure 12. The leader cells maintain a higher density of focal adhesion sites compared with that of the other cells at the wounding frontier. (A) Representative images of the focal adhesion distribution, green: vinculin, blue: nucleus83

Figure 13. The adhesions junctions form focal adhesion junctions at the leader edge of the wound. (A) the structure of VE-Cadherin and actin stress fiber distribution with in

the cell monolayer; (B)-(D) zoomed in images of the adhesions junction structure at the different locations of the monolayer.....84

Figure 14. The adhesions junctions form focal adhesion junctions at the leader edge of the wound. (A) the structure of VE-Cadherin and actin stress fiber distribution with in the cell monolayer; (B)-(D) zoomed in images of the adhesions junction structure at the different locations of the monolayer.....85

Figure 15. Modulating leader cell density via changing geometry of cell monolayer. (A) Increasing leader cell density via converging shaped cell monolayer; (B) Increasing leader cell number via diverging shaped cell monolayer; (C) Rectangular shaped cell monolayer maintains constant leader cell number and density.....89

Figure 16. Geometry of cell monolayer and migrating direction modulate leader cell density and monolayer migration rates. (A - B) leader cell density (A) and migration rates (B) variation during collective cell migration in different geometrical cell monolayers; (C – E) Comparing migration rates (C), leader cell density (D), and rate variation (E) 16 hours after wounding in different geometrical cell monolayers.....90

Figure 17. Migration rates calculated using equivalent displacement from area variation in converging (A) and diverging (B) cell monolayer migration91

Figure 18. PIV analysis indicates that the cell monolayer migration rates increase as the leader cell density getting higher. (A) Migration rates and direction distribution within the converging cell monolayer at different time points. (B) The migration rates distribution from the leading edge to the inner region of the monolayer; (C) The migration direction distribution from the leading edge to the inner region of the monolayer.....95

Figure 19. PIV analysis indicates that the cell monolayer migration rates maintain constant in diverging pattern. (A) Migration rates and direction distribution within the diverging cell monolayer at different time points. (B) The migration rates distribution from the leading edge to the inner region of the monolayer; (C) The migration direction distribution from the leading edge to the inner region of the monolayer.....96

Figure 20. Competing wound healing assay. (A) the concept of competing wound healing assay; (B) Representative images of competing wound healing assay; (C -D)

Leader cell density (C) and migration rates (D) in converging and diverging directions in competing wound healing assay.....97

Figure 21. . PIV analysis of the competing pattern. (A-B) migration rate and angle mapping on the cell monolayer; (C-D) quantitative analysis of the migration rates and angle distribution in the direction parallel with the wound leading edge.....98

Figure 22. Area ratio of cell monolayer migration toward converging and diverging directions in competing wound healing assay.....99

Figure 23. Arsenic treatment increases the cell monolayer migration rates. (A) Representative images for the cell monolayer migration in arsenic treatment and control cases; (B) Low concentration of arsenic treatment increases the cell monolayer migration rate.....112

Figure 24. PIV analysis results indicate that arsenic treatment increases the cell migration rates towards the wound leading edge. (A) Representative images for the cell monolayer migration in arsenic treatment and control cases; (B) Migration rates and angle distribution within the cell monolayer.....113

Figure 25. The low concentration arsenic treated cell monolayer developed a fast migrating leading edge compared with that of the control case115

Figure 26. Arsenic treatment increases the correlation level of cell monolayer migration. (A) the concept of correlation level; (B) correlation level of the control and arsenic treated case with the increasing the distance from the leading edge; (C) The correlation level in arsenic treated and control cell monolayer migration.....116

Figure 27. Arsenic treatment increases the correlation level and motility of integrated cell monolayer. (A) The migration direction and amplitude distribution within an integrated cell monolayer; (B) The migration rates in arsenic treated cell monolayer and control case; (C) correlation level of the arsenic treated cell monolayer and control case.....118

Figure 28. The proliferation effects on HaCaT cell monolayer reduces its effects on cell monolayer migration. (A) Low dose arsenic treatment proliferates HaCaT cell monolayer; (B) the cell monolayer with high cell density migrates slow compared with that of the cell monolayer with low cell density.....119

| | |
|--|-----|
| Figure 29. Arsenic treatment enhances the leader cell characters to driving the cell monolayer migrating forwards. (A) concepts of parameters used to characterize the leader cells; C. I., curvature index, L, contour length of wound leading edge, <i>l</i> , linear length of wound leading edge; (B-D) Representative images of leader cells in control and low dose arsenic treatment cases; (E-H) leader cell characters in arsenic treated and control cases..... | 121 |
| Figure 30. Arsenic treatment increases the expression level of stress fiber..... | 123 |
| Figure 31. Arsenic treatment condenses the focal adhesion sites at the protrusion leader cells. (A-B) representative images of vinculin distribution within cells, scale bar 50 μ m; (C) quantitative analysis of focal adhesion density at Protrusion tips and frontier of the cell monolayer | 124 |
| Figure 32. Arsenic treatment increases the expression level of E-Cadherin on the cellular boundary | 125 |
| Figure 33. Arsenic treatment increases Nrf2 and its downstream gene, HO-1, expression in a dose dependent manner. The cellular expression of E-Cadherin is not affected by arsenic treatment | 127 |

Figure 34. Western blot results indicate that Arsenic increases the Nrf2 expression level at protein level. (A). the effects of arsenic on HaCaT cells with different expression level of Nrf2; (B) the ability of arsenic regulate expression of Nrf2 varies in different Nrf2 expression level; (C) the ability of arsenic regulate monolayer migration varies in different Nrf2 expression level.....128

Figure 35. Nrf2 expression level regulates the effect of arsenic treatment on leader cells. (A – B) arsenic regulation ability on curvature index (A) and leader cell density (B) in different Nrf2 expression level. (C-E) representative images of arsenic treatment under different Nrf2 expression level.....129

Figure 36. PIV analysis of cell monolayer migration with high and low level of Nrf2 expression. (A). migration rates and migration angle mapping on cell monolayer; (B) quantitative analysis of migration rates distribution within cell monolayer; (C) quantitative analysis of migration direction distribution within cell monolayer.....132

Figure 37. Over expression of Nrf2 increases the correlation level of cell monolayer migration.....133

NOMENCLATURE

ECM: extracellular matrix

EMT: epithelial mesenchymal transition

siRNA: small interfering RNA

Bio-MEMS: biomedical microelectromechanical systems

PIV: particle imaging velocimetry

AC: alternative current

DC: direct current

HUVEC: Human Umbilical Vein Endothelial Cells

HaCaT: an immortal human keratinocyte line

TBST: Tris Buffered Saline with Tween® 20

PBST: Phosphate Buffered Saline with Tween® 20

PBS: Phosphate Buffered Saline

ROS: Reactive oxygen species

ABSTRACT

Collective cell migration is critical for various physiological and pathological processes. *In vitro* wound healing assay has been widely used to study collective cell migration due to its technical simplicity and ability of revealing the complexity of collective cell migration. This project studies the function and importance of leader cells, the cells pulling cell monolayer migrating into free space, in endothelium and skin epithelial regeneration via plasma lithography enhanced *in vitro* wound healing assay. Despite leader cells have been identified in *in vitro* wound healing assays, little is known about their regulation and function on collective cell migration. First, I investigated the role of leader cells in endothelial cell collective migration. I found that the leader cell density is positively related with the cell monolayer migration rates. Second, we used this knowledge to study the effects of arsenic treatment on skin regeneration via *in vitro* wound healing assay. We found that low concentration of arsenic treatment can accelerate the keratinocyte monolayer migration. We further found that arsenic affected cell migration by modulating leader cell density through Nrf2 signaling pathway. As a conclusion of these studies, we evaluated the function

of leader cells in collective cell migration, and elucidated the mechanism of arsenic treatment on skin regeneration.

Chapter 1

INTRODUCTION

Collective cell migration is an important and complex biological process involved in many physiological and pathological processes, such as embryogenesis and cancer metastasis. In this chapter, the status of collective cell migration in *in vitro* wound healing assay, especially the emergent leader cells, will be provided. The main hypotheses and structure of this research will also be discussed here.

1.1 Collective Cell Migration

Collective cell migration is an important and still poorly understood phenomenon associated with many significant physiological and pathological processes [1, 2]. The maintenance of cell-cell adherens junctions during cell migration is a hallmark of collective cell migration. During migration, cells are mechanically and chemically connected with each other via Cadherin involved adherens junctions. Through these connections, physical and chemical information can be spread out in the partial or whole cell groups, which affects single and collective cellular behaviors in the cell group during migration [3]. For example, during *in vitro* wound healing assay,

the information of the wounding affects not only the cells at the wound leading edge, but also the cells in the monolayer far behind the leading edge [3, 4]. The migration of cells far behind the wounding frontier can be directed by this information. Interestingly, this integrated interaction among cells induces emergent characters of the cell group which cannot be explained by characters of single cell migration. In wound healing assay, for example, a subset of cells at the wound leading edge are evolved to a leader cells type. They are exceptionally motivated, and generate more traction force to pulling the cell monolayer migrating forward via the adherens junctions [5] [6].

In multi cellular organism, many physiological and pathological processes involve collective cell migration. The cell-cell adherens junctions among cells maintain the physiological function of the cellular entity during their movement. During embryo development, a group of cells migrate to new niche to perform their predefined functions. In this complex process, the cellular chemical and mechanical interactions and the cell-ECM (extra cellular matrix) interactions guide the cells to their destinations. In zebrafish, for example, the Sdf1-Cxcr4 chemokine signaling axis guide a cohesive cell group migrating along the flank of the zebrafish embryo to develop into a mechanical sensitive organ [7]. In addition, collective cell migration is also involved

in disease development, such as cancer invasion. Tumors, tissues of tightly connected cells, invade into other tissues during cancer metastasis. In *in vitro* model, many kinds of cancer cells, such as breast cancer, and colorectal carcinoma, go through collective invasion [8]. Epithelial cancer cells can detach from the primary tumor, and migrate individually or collective into a new niche, which termed as epithelial-mesenchymal-transition (EMT) [9].

Even through the importance of collective cell migration in multicellular organisms has been recognized for a long time, the governing mechanism(s) of collective cell migration still a mystery, though single cell migration has been very well studied [10]. The dynamic process of collective cell migration involves interactions among the cells, interactions between the cells and their microenvironment, and intracellular reactions. These multi-perspective interactions determine that collective cell migration should be addressed from multiple disciplines, including mechanics[11, 12], material science[13], and biology[14].

From engineering perspective, collective cell migration can be interpreted as a multi-agent system, in which the knowledge of single cells migrating behavior alone

cannot explain the emergent system level behaviors. In *in vitro* wound healing assay, for example, the frontier of wound develops from a straight line to a curvature with multiple leader cells. These emergent leader cell phenomena cannot be explained by the governing principle of single cell migration. In addition, the traction force generated by cells not only can affect neighbor cell behavior, but also affect the cells in a large area of the monolayer [15]. This system level mechanical interaction shines light from a new perspective to interpret the behaviors of cell groups. By direct measurement of the traction force distribution within an integrated cell monolayer, the results indicated that the forces driving the cell monolayer migrating forward raised not only from the wound leading edge, but also from the inner region of the cell monolayer. The stress distribution within the cell monolayer also indicates that the local cell migration follow the orientations of the maximal principle stress direction[16].

As a summary, understanding the mechanisms of collective cell migration benefits basic research on various physiological and pathological processes, and provide insights for developing strategies for curing diseases, such as cancer. The dynamic characters of collective cell migration requires interdisciplinary cooperation involving physical sciences, material sciences, and biological sciences.

1.2 *In Vitro* Wound Healing Assay, and Emergent Leader Cells

To study collective cell migration, various models have been developed, such as Boyden chamber[17], and sprouting assays[18]. Currently, with the development of tissue engineering, the collective cell migration can be study in an environment mimic the cell microenvironment in *in vivo* conditions[19]. Among these assays, *in vitro* wound healing assays are some of the most common approaches in study collective cell migration due to their technical simplicity and ability to visually the cells during cell migration.

In vitro wound healing assay is inspired by the *in vivo* wound healing process. The integrity of epithelium is vital important for its function [20]. The endothelium, a cell monolayer in the inner surface of blood vessel, for instance, works as a barrier between the blood and smooth muscle cells around the vessel, which requires integrity. When the epithelium is damaged, in blood vessel, skin, or digest tract, the epithelial cells near the wounding region will migrate collectively to recover the damaged region[21]. In *in vitro* wound healing assay, a confluent cell monolayer is wounded either by scratching or a physical blocker to generate free space for cell

migration. To reduce the complex level of the collective cell migration, only one cell line is involved in most *in vitro* wound healing assays, in contrast to the interactions of multiple cell types in *in vivo* wound healing process.

Though simple as it is, *In vitro* wound healing assay can provide insights of collective cell migration from multiple perspectives. First, the basic mechanisms governing the wound healing process can be studied. By reducing the system from multiple cell types to single cell type, the complexity of the system is dramatically reduced and the governing principle can be studied. Two governing principles of wound healing process have been proposed based on research using *in vitro* wound healing assay: the purse-string [22] and cell protrusion methods [4]. Second, the effect of ECM, including the chemical signals and physical characters, on collective cell migration can be addressed in *in vitro* wound healing assay. Chemicals can be simply added to the medium of the cell, and their effects can be studied by observing the cell migration dynamics [23]. By manipulating the stiffness of the substrate, the physical character of the microenvironment can be studied [3]. Third, *in vitro* wound healing assay can provide information from multiple perspectives. The very basic information is the monolayer migration rates of the whole cell monolayer. To measure

the velocity distribution within in the cell monolayer at subcellular resolution, live cell imaging and cell migration tracking can be performed [24] . By measuring the velocity distribution within the monolayer, the correlation level of the cellular motion can be studied. The traction force microscopy can be used to measure the traction force distribution of within the cell monolayer [25]. Combining the information of velocity and traction force mapping in the monolayer, the dynamics of the collective cell migration can be studied. In addition, geometry of the cell monolayer can also be manipulated via biomaterial patterning and functionalization of substrate [26]. Via this method, the effects of cell monolayer geometry can be studied [27, 28]. In addition, the injury level of the cell monolayer can also be studied via the scratch or the blocker assay [29]. Another perspective is the electrical effects on collective cell migration [30]. It can be studied via generating the cell monolayer on top of electrodes [31].

Various methods have been developed to generate a precise wound and observing the collective cell migration from multiple perspectives. The basic concepts of wounding methods and their characteristics are provided in Chapter 2. Micro-fabrication techniques are also used to measure traction forces generated by the cells during wound healing process [32]. Cell patterning methods was applied to regulate

the geometry of the cell monolayer and further study the correlation between the geometry and collective cell migration [27, 33]. Overall, the *in vitro* wound healing assay is widely used due to its simplicity and functionality.

In *in vitro* wound healing assay, two governing mechanisms has been proposed to explain this dynamic collective cell migration: purse-string and cellular protrusions [4]. In the purse-string principle, the cells at wound leading edge form a connected actin bundle, and the forces generated by the actomyosin contractions pull the cell monolayer migrate towards the cell free region [34]. In the cellular protrusions principle, the cells at leading edge generate large lamellipodia, which maintain a large number of focal adhesion sites, and pull the cell monolayer migrate into the cell free region.

In *in vitro* wound healing model, the frontier cells do not migrate with the same rates. Accordingly, the leading edge of the wound evolves from a straight line to a curving shape. The cells migrating faster form leader cells and pull the cell monolayer to migrate forward [5]. These leader cells maintain unique characters to facilitate the cell migration [35]. This emergent collective phenomenon cannot be observed in single

cell migration, and also cannot be explained via the governing principles of single cell migration [5]. During the wound healing process, single cell mobility, intercellular interactions, and the cell-substrate interactions together affect the cell monolayer behavior. For this reason, to investigate emergent behaviors of cell monolayer system, a comprehensive consideration of those three perspectives should be addressed. Other than *in vitro* wound healing model, leader cell concept has been widely studied in angiogenesis process. To lead the stalk cells migration out during angiogenesis, the leader cells are single, high polarized cells with long filopodia [36]. In both angiogenesis and cell monolayer wound healing cases, the leader cells maintain characters to facilitate migration, such as highly polarized and long filopodia, intensive stress fiber. In wound healing assay, leader cells are not necessarily from the wounding leading edge. Some of them may “jump over” from the second or the third cell row behind the frontier [4], [37]. In *in vitro* wound healing assay, the physical environment also affects the leader cell formation. Mechanical pressure can increase the leader cell number, thus increase the cell monolayer migration rates accordingly [38]. The geometry of the wounding frontiers affects cell migration [39]. My results show multiple evidences for that the leader cells guide the cell monolayer migrating forward

[33]. Via the plasma lithography enhanced *in vitro* wound healing assay, my results also indicate that leader cells maintains a constant density along the wound frontier, around four leader cells per millimeter. Coincidentally, the cell migration rate maintains constant with various widths of rectangular cell monolayer patterns. Further experiments were performed to validate whether the constant leader cell density determines the stable migration rates. Different geometries of cell monolayer were used to test this hypothesis, such as rectangular pattern, and triangle pattern.

1.3 Arsenic, Collective Cell Migration, and Nrf2 Signaling Pathway

Arsenic is a well-established human carcinogen. Under some conditions, arsenic can easily dissolve into underground water [40], and affect human health through drinking water. Arsenic contaminated ground water threatens millions of people all around the world, from eastern, southeastern, southern Asia to Latin America, America, and Europe [41]. Chronically in taking high arsenic concentration drinking water may induce hyper- or hypopigmentation, peripheral neuropathy, skin cancer, bladder and lung cancers, and peripheral vascular disease [42]. Among all the cancers related with arsenic, skin cancer is the most common one [43]. Skin lesion is a sign of

in taking high concentration arsenic drinking water. Due to the carcinogenic character of arsenic, WHO reduced the safe level of arsenic concentration in drinking water from 0.05 mg/liter to 0.01 mg/liter [42].

In vitro studies show that arsenic affect EMT [44], cell migration [45], and differentiation [46]. Due to the importance of cell migration in cancer development, the effect of arsenic on cell migration may play a vital role in its toxicity. Huang et al. reported that arsenate treated HaCaT cells were larger and migrating faster [47]. By contrast, arsenic treatment reduced migration rate of H9C2 Myoblasts by reducing and redistribution of Focal adhesion [45]. However, the mechanism of these effects has not been intensively studied. Arsenic affect many signaling pathways involved in cell migration, including PI3K[48, 49], Rho[50], MEKK-JUK[51, 52], and Nrf2[53]. Among them, Nrf2 signaling transduction pathway plays a dual role in arsenic induced effects. Arsenic induced Reactive oxidative species (ROS) can stimulate cells to up regulate Nrf2 level to protect the cells from this oxidative stress [53]. In addition to its protective effect on ROS, Nrf2 is reported to regulate cell migration. Corneal epithelial cells migrate rates could be regulated accordingly by manipulating Nrf2 level [54]. While, the breast cancer cell monolayer migrates slower with high expression level of

Nrf2[55]. To elucidate the mechanism of Arsenic effects on skin cancer development and skin regeneration, the effect of arsenic on collective keratinocyte cell monolayer migration should be investigated. My results on collective cell migration on HaCaT cell, an immortalized keratinocyte, indicated that arsenic affect HaCaT cell migration in a dose dependent manner. The maximum cell migration rate at medium concentration of Sodium Arsenate, as 2 μ M. To identify the mechanisms governing this phenomenon, the cell signaling pathways and cell migration dynamics should be investigated.

1.4 Main hypothesis and structure of this research

This project aims to elucidate the roles of leader cells in endothelium and skin regeneration via plasma lithography enhanced *in vitro* wound healing assay from mechanical and biological perspectives.

I hypothesized that leader cell density positively related with the cell monolayer migration rate. To test this, I will develop a method to manipulate the leader cell density along the wound healing process using plasma lithography enhanced *in vitro* wound healing assay. The cell monolayer is patterned into a trapezoid shape and

wounded at the converging direction by removing physical blockers. As cell monolayer migrating forward, the wound leading edge will be reduced to increase the leader cell density. In this process, cell monolayer migration rate and kinetics are measured to test my hypothesis. In addition, competing assay will also be performed. In competing assay, a monolayer will be wounded in both converging and diverging directions. Cell migration rates at these two competing frontier are measured. These proposed experiments will provide concrete data to test my hypothesis.

Cancer development are related with collective cell migration [2, 56]. It is important to elucidate how carcinogen affects cancer development via collective cell migration. It is has been reported that arsenic affects skin cancer development [57], and cell migration[45]. I hypothesize that arsenic may affect the emergent leader cells in collective cell migration. To test this idea, the variation of cell migration dynamics, emergent leader cell phenotype, and molecular signaling pathways will be probed. The cell monolayer migration rates and velocity distribution within the monolayers are to be observed. The leader cells are characterized from mechanical, morphological, and molecular perspective. Treating cells with arsenic can generate hydrogen peroxide and other reactive oxidative species [58], which will up regulate the expression level of

Nrf2, the primary cellular defense mechanism against oxidative stress. Nrf2 signaling pathway also affects cell motility and migration in cell type dependent manner [59-61]. We hypothesize that the dual roles of Nrf2 on protecting cells from oxidative stress and cell migration, and the toxicity of ROS work in a system manner to affect the cell migration. To test this hypothesis, small interfering RNA (siRNA) technique is used to manipulating the Nrf2 expression level to investigate the role of Nrf2 in arsenic induced cell migration. Via silencing Nrf2 or KEAP1 gene, the Nrf2 protein expression level will be down, or up regulated. The cell monolayer migration will be observed under these siRNA gene silencing.

In long term, this research can benefit solving problems in development, regenerative medicine, and cancer biology fields. Carcinomas, cancer related with epithelial tissues, covers 80% to 90% of all cancers. Studying the collective cell monolayer migration can provide insight of development of Carcinomas. By clarify the effects of arsenic on keratinocyte monolayer migration, we may provide insight for developing therapies for skin cancer. Secondly, embryo development can also be benefited by collective cell migration study. During development, the mechanical characters of the microenvironment of cells affect the cell migration and stem cell

differentiation [62]. My study on emergent characters of collective cell migration will benefit the study *in vivo*. In the future, using the experience from this project, I will investigate the emergent characters of the cell monolayer via self-organization knowledge. Moreover, I can transfer to other models, such as angiogenesis model, and vasculogenesis model to study cell migration from mechanical perspective. Both two models also have significances in development and cancer metastasis.

As a summary, this research aims to elucidate the function of emergent leader cell characters of collective cell monolayer migration, and its significance in arsenic affecting keratinocyte migration. This research will benefit the study in embryo development, and cancer development. Using the skills and knowledge gained from this project, I can study collective cell migration in other more clinically significant models, such as angiogenesis and vasculogenesis model.

1.5 Specific aims

Aim 1: Define the role of leader cell in collective cell migration in *in vitro* wound healing model.

- A) Using rectangular cell monolayer pattern tests the relationship between the leader cell number and cell migration rate.
- B) Characterize the leader cells from multiple perspectives.
- C) Study the relationship between the leader cell density and cell migration rate by reducing the width of wound leading edge as cell migrating.
- D) Elucidate relationship between the cell monolayer migration rate and leader cell number by competing wound healing assay: generating two wound frontiers in a single monolayer in opposite directions.

Aim 2: Elucidate the effects of arsenic on keratinocyte cell monolayer collective migration in *in vitro* wound healing assay

- A) Investigating the relationship between arsenic concentration and cell monolayer dynamics (leader cell density, migration rates).

B) Investigating the role of Nrf2 signaling pathway in the effects of arsenic on HaCaT cell monolayer migration dynamics via siRNA gene silencing technique.

Chapter 2

BACKGROUND

To study collective cell migration, numerous methods has been developed, such as Boyden chamber assay[63], wound healing assay [64], and sprouting assay [65]. Among these assays, *In vitro* wound healing assay is widely used for its technical simplicity and ability to reveal the complex of collective cell migration. In this chapter, I will review the methodology of *in vitro* wound healing assay [66].

Basically, *in vitro* wound healing assay aims generate a cell free space from a confluent cell monolayer for cell migrating into. The cell migration process is observed and analyzed. Even the *in vitro* wound healing assay is a relatively simple system compared with the *in vitro* case, many events also happened during the wounding and healing processes. The cells at wounding frontier are injured, and release cytoplasm contents. These cellular proteins may affect the behavior of neighboring cells. Cell free space is generated for cell migrating into, and the substrate of this free region can be coated with proteins or cellular residues.

Due to the effects of the wound geometry on the migration process, precise wounding methods also should be developed. To achieve multiple perspective control of the wounding process, various wound healing assay have been developed to make this assay more controllable. In addition, the cell migration information from multiple perspectives should be collective to uncover the governing mechanisms of collective cell migration. In this chapter, I will review the current wounding and observing methods in *in vitro* wound healing assay.

2.1 Wounding methods

1 Mechanical wounding method

The first developed wound healing assay for studying collective cell migration is mechanical wounding assay. It is also the most widely used method for investigating collective cell migration, because of its simplicity and cost-effectiveness. In this assay, the cells are removed mechanically, and the collective migration process is observed. This assay can be grouped into scratching assay and stamping assay. In a typical scratch assay, a physical scraper scratches through an integrated cell monolayer to generate cell free region for cell migration. A scraper can be pipette leader, bladder, or

a plastic comb for generating multiple wounds at the same time [67]. To improve the repeatability and productivity, a robotic scratching system has been developed [68]. Another reproducible scratching method for collective cell migration study is the hydrophilic polydimethylsiloxane (PDMS) slab assay [69]. This assay generates the wounded monolayer near the boundary, and minimized the cell residues and surface damage of the cell free region of the substrate. In this method, a short hydrophilic PDMS slab with a desired shape is embedded onto the substrate coated with the testing materials, allowing cells to grow on top of both substrate and PDMS. After a confluent cell monolayer is formed, the removal of PDMS wounds reproducibly the cells near the boundary and allows cells to migrate onto the debris-free surface. Another example of mechanical wound healing assay is stamp assay. Herein, a stamp punches onto an integrated cell monolayer to generate cell free region. The geometry of the wounding cell free region can be well controlled by designing the shape of stamp. Another benefit of this assay is that cellular residues are left on the cell free region, thus chemotactic chemicals could be released from cytoplasm and affect the behavior of neighbor cells [70].

2 Physical blockers assay

Physical blockers are used to generate cell free region without cell residues for collective cell migration. Rather than remove cells for generating cell free region, a physical blockers is applied to block cell attachment after cell seeding. A physical blocker is placed onto the substrate before cell seeding to block cell attachment, and the removal of the physical barrier initiates the cell migration process. This method has several benefits. It increases the repeatability of wound healing assay compared with scratch assay. In physical blocker assay, the wounding process damages minimally the cells in monolayer compared with mechanical wounding assay. Thus, this method can be used to study collective cell migration in which the cells are not injured, such as cancer invasion. In addition, this method keeps the cell free region intact from ECM deposition. This could allow investigation of different molecular mechanisms and signaling pathways underlying cell migration and elucidation of the specific functions of ECM components and growth factors. Two blockers assay have been developed: solid blocker and liquid blocker assays. In solid blocker assay, the blockers are composed by biocompatible materials, such as Teflon [71, 72] and PDMS. In this assay, the blocker is placed onto the substrate and then cells are seeded; after forming intact monolayer, the blocker is removed and cells initiate to migrate into cell

free region. The blockers can be hollow or closed geometry. The closed shape blocker generate a connected cell free space, while in hollow blocker, the cell free space can be separated [72]. The hollow shape blocker, such as a circular ring, cells can be seeded into the inner and outer compartments and migrate into the cell free space between this two cell monolayers. Liquid stopper is another blocker assay using liquid or gel in outward cell migration and proliferation assays. One of the first liquid blocker assay uses agarose gel. Cells are first centrifuged to pellets, and then introduced to agarose gel. A droplet of agarose gel-cell solution is delivered into a micro plate well surface and cooled down until the gel solidified. The medium then added into the well, and the cells are incubated for cell migration study. This method can generate cell monolayer boundary without injury, and the cell-substrate interaction can be controlled by coating materials of interest onto the well plate.

3 Chemical method

Toxic chemicals can also be used to wound the integrated monolayer. Sodium hydroxide, for example, can wound the cell monolayer by lysing cells and create model wounds chemically [73]. In this method, a droplet of sodium hydroxide is placed onto

the cell monolayer, and the cells contact with sodium hydroxide are removed. The location and size of wound are controlled by the position of pipette and the volume of the chemical solution. To precisely control the wounding location and study the effects of liquid flow on wound healing process, a microfluidic wound healing system has been developed. The device consists a micro channel with three inlets. According to the wounding location and size of the wound, trypsin solution flow through 1 or 2 inlets with other inlets running medium during wounding process. The trypsin solution removed the cells contacted with it. In the healing process, all channels run medium or other chemicals under test. Because the flow in micro scale is laminar, the wounding frontier can be controlled precisely. To improve the efficiency of experiment, a multi-channel wound healing device has been developed. This system has 24 channels, and can be controlled by computer program to improve the throughput. The micro channel also allows cell stimulation mechanically or chemically during the wounding process. In particular, fluid flow can be applied to investigate the role of shear stress in wound healing, and chemical gradients can be created in the micro channel to study their chemotactic potentials [74].

4 Electrical method

In contrast with mechanical wounding methods, electrical wounding methods, based on the electrical cell–substrate impedance sensing (ECSI) technique, can create wounds with different geometries and measure the electric impedance of the cell monolayer, which indicates the cell movement. The electrical wound-healing system typically is composed of a working electrode for cell adhesion and a counter electrode. By applying a relatively large voltage between the electrodes, the cells on the electrode can be electropermeablized permanently to generate a model wound in the monolayer [75]. After wounding, the variation of impedance on the cell–adhesion electrode is recorded to monitor the cell migration. Because of the insulating property of the cell plasma and membrane, the cell movement can be characterized by measuring the electric impedance of the cell monolayer. The wounding and measurement processes can be strongly influenced by the electric signals applied between the electrodes. For example, the polarity of the cell–adhesion electrode determines the wounding characteristics if a direct-current (DC) pulse is applied [31]. If the cell adhesion electrode is positive, the cell wounding is extended beyond the electrode. If the polarity inverses, it will result in a higher uncertainty in the impedance measurement. A high-

frequency AC signal can be applied to improve the electrical wounding method. With AC electric potential, the cells permanently electroporated can be confined on the electrode. Besides the electroporation principle, the electrical wound methods can also be combined with the physical blocker assay to generate a cell-free area for collective cell migration. In addition, a self-assembled inhibitive monolayer can block the cell from settling onto the electrode after cell seeding. When the cell sheet is confluent and the cell edge forms around the electrode, a DC signal is applied to remove the inhibitive monolayer due to the electrothermal effect. After that, the cells are able to migrate onto the cell-free electrode. Compared with electroporomeablization, this method can exclude the cell debris in the cell-free region. A major advantage of the electrical method is the ability to automate the process for high-throughput study. An array of wounds can be monitored simultaneously and automatically based on the impedance. This can significantly increase the throughput compared with manual optical characterization with a microscope.

5 Optical method

Light also can be used to generate a wound in a cell monolayer. A laser beam exert a physical force onto the surface it radiating. This photomechanical phenomenon can wound the cell monolayer by killing the cells it radiating. Using this method, the wounding process can be precisely controlled by program, which enhances the throughput of this method. Other advantages of optical wounding methods include the ability to create repeatable wounds, create wounds with arbitrary shapes, and perform automated microscopic observation using the optical interface [76, 77].

6 Cell monolayer geometry control in wound healing assay

Previous results indicate that geometry of cell monolayer affect various characters of biological system. For example, the geometry of the cell monolayer affects the endogenous stress distribution within the cell monolayer [78]. In addition, the geometrical confinement can regulate the cell migration modes [79], and proliferation [80]. The substrates can be coated with fibronectin with micro-contact printing to pattern the geometry of the cell monolayer. Via plasma lithography, selectively treating the polystyrene substrate with air plasma, the cell monolayer can be patterned as the predesigned geometry [13].

2.2 Observation methods in wound healing assay

1 Traction force measurement in wound healing assay

Collective cell migration can be interpreted as dynamic mechanical process. The stresses among cells and between cells and substrate are important information to interpret the mechanical principles of collective cell migration. Two methods has been developed to measure the force/stress distribution of the cell monolayer during wound healing process. The first method is traction force microscopy. Basically, this method tracking the displacement of fluorescent beads, and combined with the elastic stiffness of the substrate to calculate the traction force cells exert onto the substrate [81]. Another method senses the traction force via measuring the displacement of micro pillars. The cell monolayer substrate is composed by an array of micro-pillars made by micro fabrication technique. Cells are seeded onto the top of pillars. During cell migration, the contraction force generated by cells deforms the pillar. By measuring the deformation and mechanical stiffness of the micro pillar, the traction force exerted by cells onto the substrate can be calculated [82].

2 cell tracking in wound healing assay

The collective cell migration dynamics within the cell monolayer offers insights of the governing principles of dynamics of cell monolayer. The most commonly used cell monolayer motion tracking method is time sequence imaging. After the cell monolayer initiates the healing process, the cell monolayer is recorded at specific time to recording the cell movement. By calculating the area cell monolayer covered or the distance the cell monolayer leading migrated, the migration rate of cell monolayer can be calculated. Simple this method is, the migration velocity of the cells within the monolayer cannot be resolved using this method. To observe the motion of cells within the monolayer, various movement tracking methods has been developed. To measure the cell motion within monolayer, a cell monolayer migration should be recorded within a time resolution at minute level, and with absolute locations of the cell monolayer. Thus, the live cell imaging technique was developed. A microscope chamber with environment control was used to culturing the cell on a microscope stage for a long time. The environment within the chamber was controlled the same as that of the tissue incubator. With the live cell imaging video, various cell motion tracking methods can be used to calculate the cell movement. The particle imaging velocimetry, a method developed to tracking particles movement in fluids, can be used to tracking

the movement of cells within the monolayer [83, 84]. In this method, two images at different time points are compared. Each image is divided into specific small units with the user defined resolution. For each unit in the first image, its counterpart is searched in the neighbor of the same location of the next image within a predefined search domain. The distance of the original unit in the first image and its counterpart in the second image was calculated. Combining with the time resolution, the velocity of this unit can be calculated. Another widely used method is the cell tracker. In this method, each cell in the cell monolayer was identified in each image, and the location of its counterpart in the second image was calculated. The benefit of this method is that this method tracks each individual cells, rather than subcellular patterns in the first method. With the calculated migration velocity, many parameters can be calculated, such as the migration speed and angle for each cell and at each time point. This migration velocity mapping, combined with the stress mapping within the cell monolayer, can provide mechanical insights of the collective cell migration.

2.3 Summary

In vitro wound healing assay was widely used to study the collective cell migration. With the advances of micro fabrication techniques, the wounding process can be controlled more precisely, and more information can be recorded, such as electrical impedance, velocity distribution, and cell traction force mapping within the cell monolayer. These experimental advances enable the scientists to tackle more complex scientific problems.

Chapter 3

METHODS

Due to the multidisciplinary character of this study, research methods from mechanical engineering, bio-MEMS, and cell biology fields were used in this study. To geometrically confine the cell monolayer, micro-fabrication method was used. To study the biology of collective cell migration, cell culture, immunofluorescence staining, western blot, siRNA gene silencing was utilized. To investigate the migration dynamics, cell traction method, Particle image velocimetry (PIV) analysis and quantitative data processing methods were involved in this study. Here I listed the research methods used in this study.

3.1. Cell culture

Two cell lines were used in this research project: Human Umbilical Vein Endothelial Cells (HUVEC) was used to study the collective cell migration in geometrical confined cell monolayer. An immortal human keratinocyte line, HaCaT, was used to study the arsenic effects on collective keratinocyte monolayer migration. Both of these cells were cultured in standard tissue culture incubator, maintaining a

37 °C and 5% CO₂ condition. The HUVEC cells are were commercially obtained from BD biosciences (HUVEC-2, 354151). Cells were cultured in medium 200 (M200-500) with low serum growth supplement (S00310) from life technologies, and 0.1% gentamicin (GIBCO). Culture medium was renewed every two days. HUVEC cells were used from passage 2 to 8. HaCaT cell was cultured in high glucose DMEM (MT-10-013-CV) base medium with 10% fatal bovine serum (Gemini, 100-106H). The medium was changed every two days, and cells were sub cultured every 3-4 days.

3.2. *In vitro* wound healing assay

In the HaCaT research, the cells are seeded into the 35 mm cell culture dish or a 24 well plate with appropriate cell density to form confluent cell monolayer immediately after their adhering to the substrate. After the cells are settled down to the substrate, arsenic with suitable concentrations are added to the wells. Incubating cells with arsenic for 24 hours, the cell monolayers are scratched using a pipette tip. The cell monolayers were imaged 30 minutes after wounding, and 3 hours thereafter. The migration rate are calculated by measuring the gap reduction between the two wound frontiers in the same location. The migration rates are calculate following the equation:

$$\text{Rate} = \frac{\Delta \text{Area}}{W * T}$$

W , the width of the measuring region; T , time interval between the two images.

To study the leader cell formation, the physical blocker assay has been used. Before seeding cells, a physical blockers, a PDMS thin layer with appropriate size were placed onto the substrate. After the cells monolayer formed following the cell seeding, arsenic with suitable concentrations was added into the dish. Incubating for 20-24 hours, the PDMS blockers were removed and cell migration was observed in the same manner as the in the scratch assay.

3.3 Plasma lithography enhanced wound healing assay

In order to study cell migration behavior with geometrical confinement, the cell monolayer geometry should be controlled. In this study, this has been achieved by creating a spatial templates of cell responsive surface chemistry on substrate. This surface functionalization method was termed as plasma lithography [13, 85-88]. Plasma lithography uses selective shielding from plasma treatment to surface contact to generate the chemical pattern on the surface. To achieve this, a PDMS mold with 3-D structures is placed in conformal contact with a substrate and exposed to air plasma.

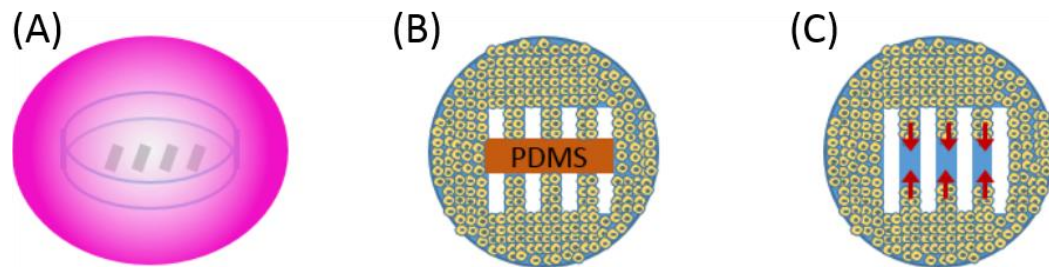


Figure 1. Plasma lithography enhanced *in vitro* wound healing assay.

(A) Plasma lithography to generate the selectively functionalized substrate; (B) cell seeding; after placed the DPMS blockers, cells are seeded into the petri dish; (C) Wounding and observing the healing process; after the cell monolayer is formed, the PDMS blockers are removed and cell migration is recorded.

Due to physical channels formed between the 3-D structure in the mold and the substrate, the substrate material is selectively, and chemically functionalized via air plasma. This selective functionalized substrate serve as a mold to confine cell monolayer in predesigned geometry. After placing the PDMS mold, the location of PDMS blockers were marked on the outer surface of the dish via a razor. In this study, the untreated, initially hydrophobic polystyrene petri dishes were plasma treated for 5 minutes with air plasma at 150 Pa and a power of 30W in a plasma cleaner. After that, the dish was placed in biosafety hood for following steps. After removing the PDMS mold, the PDMS blockers are placed on the marked position. Then cells are seeded into the dish. Several wound healing assays were used in this study. For the scratch assay, cells were seeded into tissue culture dish or 24-well plate wells with 6×10^4 /mm². A wound is generated by scrapping in the center of an integrated cell monolayer via a sterilized pipette tip. The cell migration into the cell free region was observed. In the PDMS blocker assay, PDMS thin layer was prepared in a petri dish at 10:1 precursor and curer reagent ratio, then baked on hot plate for 4 hours at 65 °C. PDMS blockers were cut using a blade (Ace hardware) sterilized with 70% ethanol to the appropriate size. The PDMS blockers were placed in the dish or 24 well plate before cell seeding.

Tweezers were used to confirm the conformal contact of the dish substrate and PDMS blockers to avoid the cells entering into the space underneath the blockers. After an integrated cell monolayer was formed, the blocker was removed. The process of cell migrating into the cell free region was observed. PDMS lift-off process should be performed carefully to avoid injuring the boundary cells. The collective cell migration process was imaged 30 minutes after removing the PDMS blockers or scratch, then being imaged every specific hours according the experiment. Cell monolayer migration rates are calculated using the same method described in the wound healing method. The PDMS mold used in the plasma lithography were fabricated using micro fabrication technique. The pattern was designed in AutoCAD software, and then delivered to commercial company to make the photolithography masks. The pattern was first transferred from the mask to silicon wafer through photolithography process in cleanroom. The PDMS was mixed with base and reagent ratio as 10:1. After mixing and degasing, the PDMS solution and poured onto the silicon wafer with the pattern, and placed onto a hot plate for at least 4 hours at 70 °C.

3.4. Immunofluorescence staining

Cells were stained for F-actin with Alexa Fluor® 555 tagged phalloidin (Life technologies), for vinculin to observe focal adhesions with monoclonal anti-vinculin antibody (Sigma Aldrich, V9131-100UL), for VE-Cadherin to mark adhesion junctions with VE-Cadherin rabbit monoclonal antibody (cell signaling technology, #2500). The nucleus was stained with ProLong® Gold Antifade Reagent with DAPI (Invitrogen, P-36931). All antibody was diluted using antibody dilution buffer (Ventana, ADB250) with the concentration recommended in the manual. The secondary antibodies with fluorescence dye was goat anti mouse with Alexa fluor 488 (life technologies, A-11001), and goat anti rabbit with Alexa fluor 488 (life technologies, A-11008). Samples were fixed with 4% paraformaldehyde (Electron Microscopy Sciences, #15714) for 10 minutes after rinsed with warmed PBS for 2 times. The paraformaldehyde was freshly diluted within one week before the experiment. The samples were then permeabilized with 0.1% triton-x 100 (Sigma Aldrich, #93443-100ML) for 15 minutes. To reduce the non-specific binding, the samples were blocked in 5% goat serum for 45 minutes. After that the sample was incubated with primary antibody for 1 hour. Following that, the sample was washed with PBST (0.05% of tween-20) for three times, and 5 minutes each time. The secondary antibody was

incubated then for 1 hour with 3 times PBST wash for 5 minutes each time. The solution in the sample was removed and the sample was air dried. Then ProLong® Gold Antifade Reagent with DAPI was dropped onto the sample with appropriate volume to cover the whole sample after it covered by glass cover slides. The boundary of the glass cover slide was sealed with nail polish (grocery store). After incubating the sample in room temperature for 24 hours, the sample was observed under microscope, Nikon 2000, and images were captured by CCD camera. The images were further analyzed via ImageJ software (NIH).

For staining with HaCaT samples, for E-Cadherin, the samples were fixed and permeabilized through incubating in ice cold Methanol and Acetone (1:1) solution in -20 freezer for 10 minutes. Then the protocol described above was used. For staining the Actin stress fiber, the sample was fixed with 4% PFA, and permeabilized with 1% triton-X 100 for 30 minutes. The protocol described above was used after that.

3.5. PIV analysis and post-analysis data processing

To study the velocity distribution within the cell monolayer, PIV analysis was performed. First, the collective cell migration process was recorded via live cell

imaging. Cell migration were observed by place the sample into a microscope stage with a 37 °C and 5% CO² environment. Cellular motion was captured through phase imaging by Nikon T2000 microscope with 10x lens. The captured time sequence images were analyzed using JPIV (13). The interrogation window was selected as the size of each cell within the images. Two passes PIV analysis was performed with 3x3 median filter between the passes. To reduce the noise level, 3x3 median filter was used after the PIV analysis. The migration speed and angle was calculated from the PIV results: the migration rate in both X and Y directions via the equation listed below:

$$Speed = \sqrt{(dx)^2 + (dy)^2}$$

$$angle = \tan^{-1} \frac{dy}{dx}$$

Here, dx and dy mean the migration rates towards the wounding frontier and perpendicular to the wounding frontier.

The correlation level was calculated in HaCaT project. The method was inspired by the reference [3]. Via the PIV data, the correlation level between two

regions were performed. Between two units of the PIV analysis, the correlation level was defined by the following function:

$$C = \frac{\langle V_i \cdot V_j \rangle}{\sqrt{\langle V_i^2 \rangle \langle V_j^2 \rangle}}$$

The function can evaluate the correlation decay at time point t for a region with d from the wound frontier. The distance between the two calculation regions also can be changed to study the spatial distribution of correlation level.

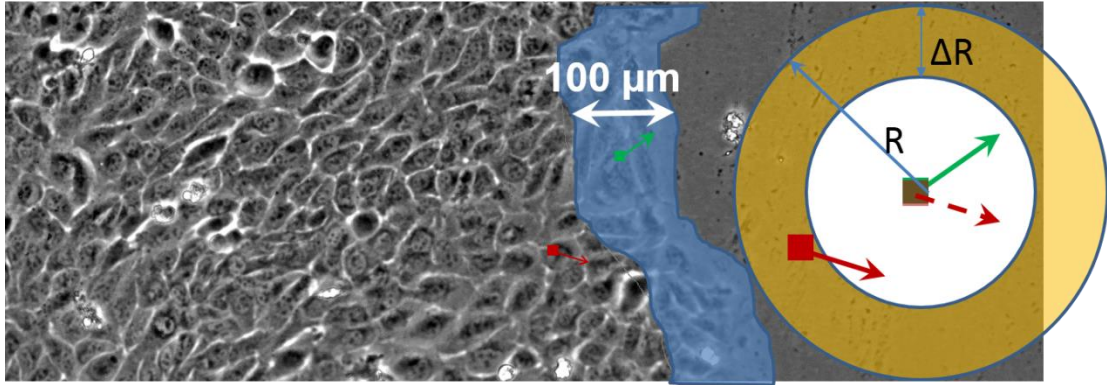


Figure 2. The concept of the correlation level in cell monolayer migration. The correlation level between the wound leading edge area with 100 μm deep and the area of R μm distance and ΔR deep. For each unit in the frontier area, the correlation between

it and each units in the following area was calculated. Then the final correlation level for distance R is the average correlation value of all units in the frontier.

3.6. siRNA gene silencing

To study the role of Nrf2 signaling pathway in arsenic induced increasing of cell monolayer migration, siRNA gene silence technique was used to manipulate the expression level Nrf2 protein. The siRNAs were purchased from Qiagen with Hs_NFE2L2_5 FlexiTube siRNA (SI03187289), Hs_KEAP1_2 FlexiTube siRNA (SI00451675), and negative control siRNA (1027310). Basically the siRNA gene silence assay followed the protocol from company. For incorporation with the wound healing assay, both the incubation time of siRNAs and arsenic are optimized. The detailed siRNA wound healing assay was described here:

On the day of transfection, appropriate density of HaCaT are seeded to form a confluent cell monolayer three days after cell seeding (before wounding the cell monolayer). The siRNA mixture solution was made according to the optimized condition, 10 nM siRNA, 3 μ l Hiperfect transfection reagent, and 100 μ l Opti-MEM (life technologies, 11058-021) for a 24 well plate well. For each 24-well plate well,

the components of the siRNA transfection solution includes: 100 μ l Opti-MEM, 3 μ l Hiperfect transfection reagent (Qiagen, 301705), and 0.6 μ l 10 mM siRNA stocking solution. Incubating in room temperature for 10 minutes, the siRNA mixture was added to the wells with cells. Incubating the cells for 40 hours, arsenic solution was added to the well, and incubated for 20 hours more. The following steps were the same as normal wound healing assay.

3.7. Western blot assay

To measure the protein expression level in HaCaT cells, and to verify the effectiveness of siRNA transfection, the western blot assay was performed. This assay mainly includes four steps: protein harvest, electrophoresis, transferring of protein and staining, and imaging. The cells were collected when the cells are at the condition to measure the protein expression. The protein concentration was measured via BCA assay to guarantee the loading of protein during electrophoresis are the same. The protein samples are mixed with loading buffer, and loaded to the wells of gel. Then the protein are transferred from gel to the PVDF membrane for immunofluorescence

staining. After staining, the last step is imaging the sample. The detailed steps were provided here:

7.1. Cell harvest

The RIPA lysis buffer system is commercial available (Santa Cruz Biotechnology, sc-24948). Raising the cells with PBS twice, the lysis buffer was added into the wells with samples. For each 6-well plate well, 100 μ l lysis buffer is added. Incubating the cells in room temperature for 1 minute, the cells are harvest using a cell scraper into a centrifuge tube. Then the cell lysis was mixed via a syringe to the sample in mucus state. The protein samples were centrifuge at 12000 rpm for 10minutes. Remove the supernatant. The protein samples can be kept for long time in -80 freezer.

7.2 Electrophoresis

Before electrophoresis, the concentration of protein in each sample should be measured via BCA assay by following the protocol from the company (Santa cruz biotechnology, sc-202389). The loading protein solution was made according to the concentration of the sample. By adjusting the loading volume of sample, the protein in each loading sample maintains at the same concentration. Loading solution including

protein sample, loading buffer, and water. The loading sample were heated up to 95 °C for 10 minutes to denature the protein. Load 20 µl onto SDS-PAGE gel, and run the electrophoresis for 1 hour at 110 V. When the protein samples located at the bottom of the gel, stop electrophoresis and transfer the protein from the gel into PVDF membrane for 1.5 hours and at 200 mA. Then the membrane with proteins are blocked using 5% nonfat dry milk in TBST solution. After blocking, the membrane was incubated in primary antibody for overnight at 4 °C fridge. After raising with PBST 3 times for 5 minutes each, the samples were incubated in secondary antibody for 1 hour in room temperature. After that, the samples are raised with PBST for 3 times and 5 minutes each time. The sample is ready for imaging.

Chapter 4

EMERGENT LEADER CELLS GUIDE ENDOTHELIAL CELL MONOLAYER MIGRATION IN *IN VITRO* WOUND HEALING ASSAY

4.1. Introduction and objective

The collective cell migration is a dynamic process involved in many physiological and pathological phenomena, including wound healing, morphogenesis, and tumor development [2]. Particularly, to maintain the integrity of endothelium, a specific epithelium lies in the inner layer of the blood vessel, endothelial cells will migrate collectively towards the wounded region to heal the gap [89]. Two governing mechanisms of collective cell migration during *in vitro* wound healing process have been proposed: purse-string [90] and lamellipodia crawling [4]. According to the purse-string mechanism, an actomyosin cable is developed along the wound leading edge, and the contraction force generated by this cable pulls the cell monolayer forward to heal the gap. In the lamellipodia crawling mechanism, the cells at leading edge develop large lamellipodia and actively migrate forward to heal the gap. In *in vitro* wound healing assay, the lamellipodia crawling has been observed more frequently.

During the active crawling process, a sub group of the wounding leading edge cells will emerge to be an active cell phenotype, leader cells [5, 91-93]. Intensive study has been performed on emergent leader cells due to its importance during collective cell migration [94]. The mechanism for developing leader cells cannot be explained solely by the principles of single cell migration [95], since the leader cells are emergent results of the interactions among the cells in the monolayer. The RhoA signaling pathway and the mechanical interactions among cells affect the formation of leader cells [96]. The polarizing cytoskeletal tension can induce leader cells in collective cell migration [91]. In addition, the leader cells are not necessarily from the leading edge; cells several layers behind the leading edge may emerge to be leader cells [4].

With the advances on the formation and function of leader cells, it has been proposed for a long time that the leader cells pull the cell monolayer migrating forward. However, a quantitative analysis of the relationship between the leader cells and the characters of cell monolayer migration is lacked. How does the quantity and density of the leader cells affect their role in regulating collective cell migration? To address these questions, the effects of leader cell density on collective cell migration has been probed. We first developed a geometrical confined wound healing assay using plasma

lithography [13, 33, 87]. Using this method, the geometry of the cell monolayer can be manipulated by selectively changing the hydrophobicity of the polystyrene substrate. Our results indicate that the cell monolayer migration rates and leader cell density (#/mm) are robust relative to the width of the rectangular cell monolayer, while it has been reported that narrower width can induce emerging mode of collective cell migration [79]. By regulating the geometry of the cell monolayer, the leader cell density can be manipulated. Via this technique, we further found that the leader cell density can regulate the dynamics of cell monolayer migration. Increasing the leader cell density can enhance the cell monolayer migration rates and the correlation level of the cells in the cell monolayer. This research identified that the leader cell density is robust and leader cells guide the follower cells in the monolayer migrating forward. These results inspire further study on the self-organizing mechanism to determine the leader cell density, which can elucidate the general governing principles of collective cell migration, and benefit tissue engineering to develop artificial tissues and organs.

Results:

4.2 Injury level do not affect the cell monolayer migration rates

We first tested the injury level effects on collective cell migration [69]. Two wound healing assays has been developed: scratch assay and PDMS blocker assay. In scratch assay, after plasma lithography, cells are seeded into the plasma treated petri dish. Cell monolayer is wounded via a pipette tip scratch. The difference of these two assays is that cell residues are left on the cell free region in scratch assay, while the cell free region is intact, plasma treated polystyrene substrate in PDMS blocker assay. Since the cell residues left intracellular proteins on the substrate, which might enhance the cell-substrate interactions, I first hypothesized that the cells in scratch assay should migrate faster than that in the physical blocker assay. I tested this hypothesis with and without geometrical control. The results indicated no significant differences of cell migration rates in PDMS blocker and scratch assay. (Figure 3).

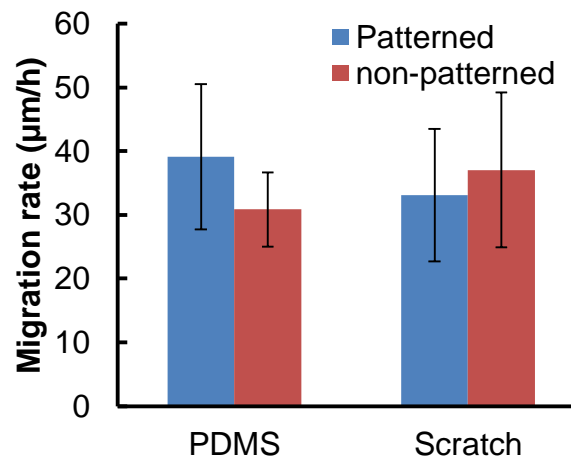


Figure 3. Injury level do not affect the cell monolayer migration rates in cell monolayer with and without geometrical confinement.

4.3 Leader cell density and cell monolayer migration rates are robust relatively to the width of the rectangular cell monolayer

To probe the relationship between leader cell density and cell monolayer migration, a plasma lithography enhanced *in vitro* wound healing assay is developed to generate geometrical confined cell monolayer for wound healing. In this method, a Polydimethylsiloxane (PDMS) mold made by micro-fabrication technique shields specific region of a petri dish substrate. The predesigned patterns are transferred from PDMS mold onto the petri dish substrate by selective protection from air plasma treatment. After placing the physical PDMS blockers onto the appropriate location, cells are seeded into the dish with appropriate density. After incubating for several hours, the cell monolayer is formed with predesigned geometry. By moving the physical blockers, the cell monolayer migrates towards the cell-free region, and this process is observed (Figure 4 A, and B). Detailed description of this method is provided in Chapter Three.

The cell monolayer was first patterned into rectangular shape to probe whether the width of the cell monolayer affects monolayer migration (Figure 4 B). We found

that the cell monolayer migration rates were constant within first 10 hours after wounding. In addition, the migration rates are robust to the variation of widths of the cell monolayer geometries, around 30 $\mu\text{m}/\text{h}$ (Figure 4 B, Figure 5 A). We further observed that the cells at the leading edge migrated unevenly. A portion of leading edge cells migrate faster and maintain different phenotypes from the others cells both at the leading edge and inner region. It has been proposed for a long time that leader cells at the frontier play an important role in cell monolayer migration [5, 6, 14]. We then hypothesized that the amount of leader cell might be related with cell migration rates. By counting the number of leader cells, we found that the leader cell number was positively related with the widths of the cell monolayer, and its density maintain constant in various widths (Figure 5 B). The leader cells located at the leading edge maintains the same characters to facilitate cell migration (Figure 6). The widths of the rectangular cell monolayer for counting leader cells range from 75 μm to 550 μm . for 75 μm , the leader cell number is smaller than 1. This is because in some cases of the 75 μm pattern, there is no leader cell. We measured the velocity distribution within the cell monolayer during collective cell migration in rectangular pattern using PIV technique. As shown in Figure 9, the cells at leading edge was separated to three groups,

according to the migration velocity. In each group, the cells are coordinated migrating towards the leading edge, and cell monolayer migration rates are higher compared with other region in the cell monolayer.

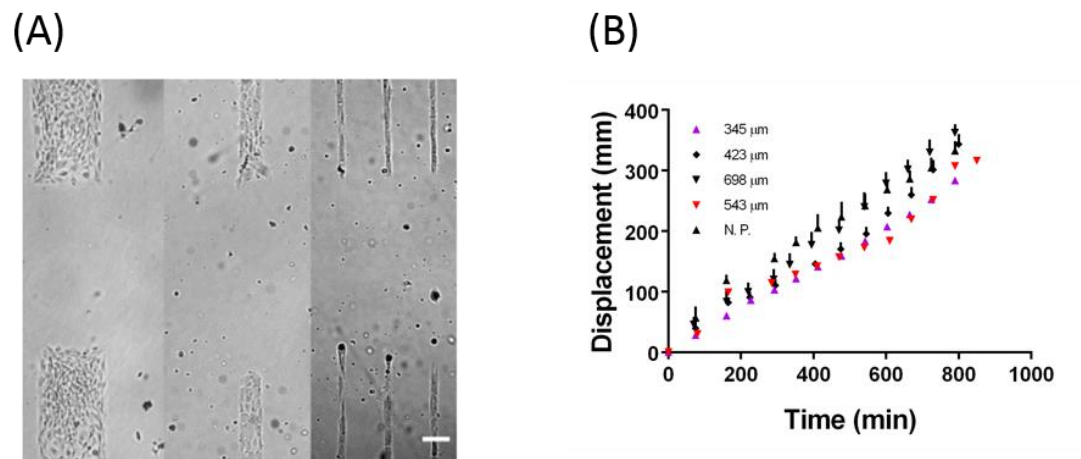


Figure 4. The cell monolayer migration rates are constant within first 10 hours after wounding. (A) Representative images of plasma lithography enhanced wound healing assay, scale bar, 100 μm ; (B) The relationship of displacements of the wounding leading edge and time after wounding.

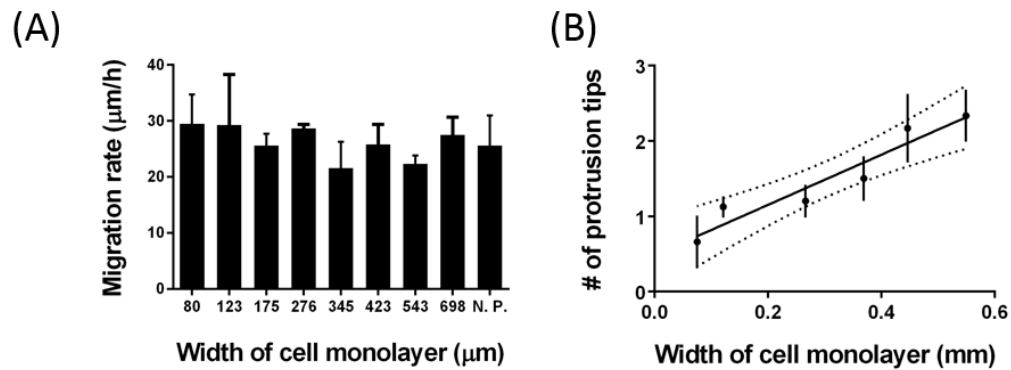


Figure 5. The cell monolayer migration rates and the number of leader cells are constant with various widths of the rectangular patterns. (A) Cell monolayer migration rates under various widths of rectangular cell monolayer migration; (B) The leader cell number is linear proportional to the width of the rectangular cell monolayer. The dashed line representative to the 95% confidential interval.

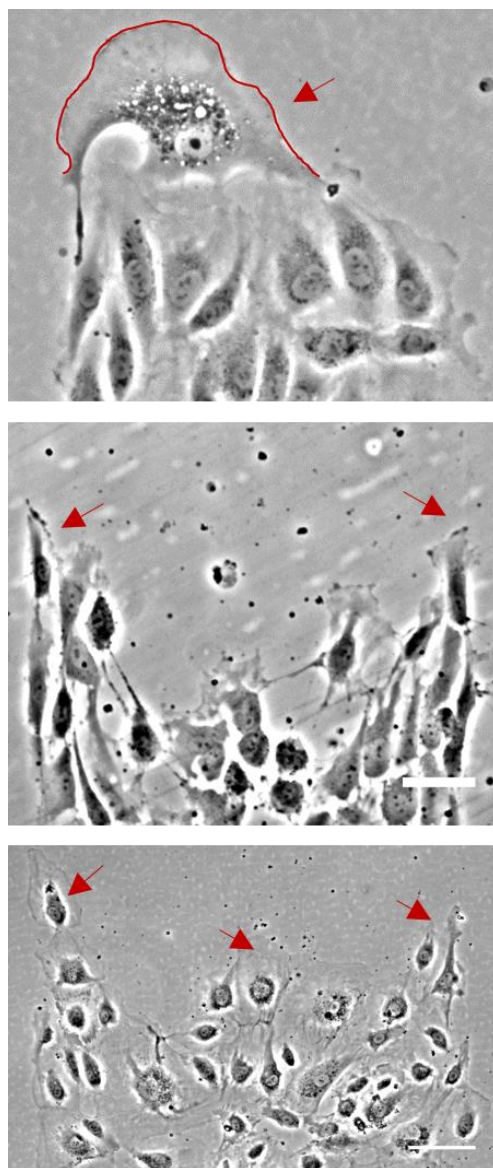


Figure 6. Representative images of the leader cells in rectangular cell monolayers with various widths. Scale bar 50 μm .

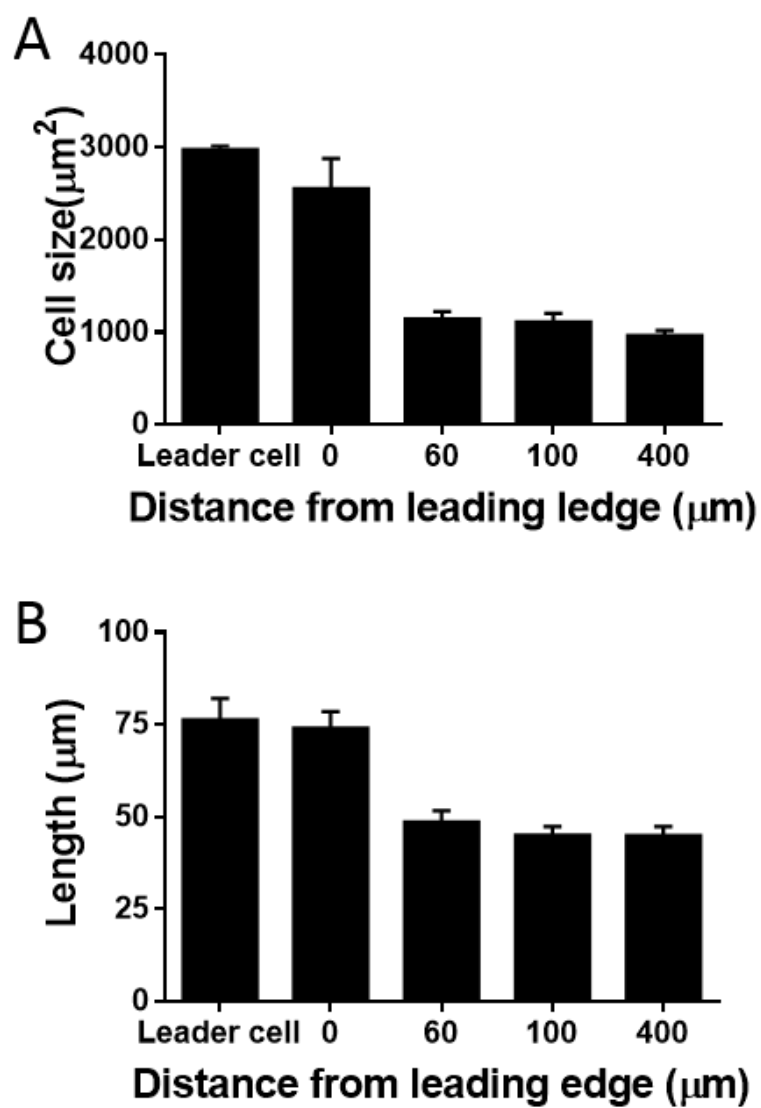


Figure 7. The size and length of frontier cells are significantly different from the cells in the inner region of the cell monolayer.

4.4 Leader cells guide the cell monolayer migrating towards the cell-free region

The leader cells are morphologically distinctive to the cells located in the other region of the cell monolayer. The free perimeter of cells provides the space for cells to develop lamellipodia to generate traction force for cell migration[38]. Quantitative measurements indicate that the leader cells maintain a free perimeter two folds longer than that of the other frontier cells (Figure 8). In addition, cells at the leading edge are two fold larger than that of cells in the inner region of monolayer. The leader cells are also larger compared with the other frontier cells (Figure 7). We also measured the length of the cells at various locations. The spindle like morphology is significant character of the mesenchymal cell, different from the epithelial cell. The cells at the frontier are much more elongated compared with that of the cells in inner region. However, the difference between lead cells and other frontier cells cannot be identified (Figure 7).

To further characterizing the leader cells from kinetic perspective, the migration velocity distribution within the cell monolayer were also measured via particle imaging velocimetry (PIV) [6]. Results clearly shown that the frontier cells migrated unevenly, even at instantaneous scale (Figure 9). The frontier cells are fell into different groups according to the migration velocity. The distance between groups is in the same level with the distance between two leader cells, around 250 μm . During its advances, the cell monolayer gradually developed a fast migrating frontier. The migration rates

decreases from the frontier to the inner region of the cell monolayer (Figure 9). The leader cells were more active compared with other frontier cells and cells in the inner region. In addition, the distribution of leader cells within the leading edge were also investigated. By counting the location of leader cells within rectangular shaped cell monolayer, we found leader cells have a high frequency located at the boundary, compared with the inner region (Figure 10). Coincidentally, the cells at the boundary migrate faster compared within the cell in the inner region.

Besides the morphological and kinetic distinctions of leader cells from other cells, leader cells maintain active characters and pulls the follower cells indicated by the molecular structure of cytoskeleton, adherens junctions and focal adhesions. To understand collective cell migration from physical perspective, actomyosin (the main source of cellular traction force), focal adhesions (the cell-substrate interactions), and adherens junctions (cell-cell interactions) were characterized via immunofluorescence imaging. The actomyosin contraction generates forces for cell migration [97]. Thus, the direction of actin stress fiber serves as an indicator of the direction of generated traction force, and an indicator for the cell migrating direction. We found that the angle between the direction from follower cell to the leader cell and the direction of the actin stress fiber of follower cells increases as the distance from the follower cells to the leader cell increases. This angle is around 45 degree when the distance is about 300 μm . This indicates that the leader cells influence the migration and contraction force direction of the follower cells, and its active region is in the same scale of the distance

between two leader cells (Figure 11 C). In addition, we found that leader cells expressed more actin stress fiber compared with the other cells in the monolayer (Figure 11 B). Focal adhesions, macromolecular assemblies, enable the interactions between the cells and extracellular matrix (ECM) during cell migration. It has been reported that the mechanical stress can affect the expression of focal adhesion [96]. By staining vinculin, a molecule involved in focal adhesion, we found that the leader cells maintain a high focal adhesion sites density (#/100 μm) (Figure 12). Combined with the larger free perimeter of leader cells, the leader cells maintain a larger quantity of focal adhesion sites compared with other leading edge cells (Figure 12). The endothelial cells in a monolayer are connected via adherens junctions involving VE-Cadherin molecule. This connection can transmit chemical and mechanical information [98] between the connected cells. It has been reported that discontinuous cell adhesion can exist among cells with high intercellular stress, and this structure was named as focal adherens junctions [99, 100]. We stained VE-Cadherin and actin fiber simultaneously at the leading edge and inner region of the cell monolayer, 8 to 10 hours after wounding. This focal adherens junctions mainly located between the leader cell and its follower cells. While at other leading edge cells and cells in the inner region, the cellular junction maintains a thin linear morphology along the cell-cell interface (Figure 13). The focal adherens junctions at the leader cells are two folds higher than that of the other leading edge cells, and four folds higher than that of the inner region cell (Figure 14).

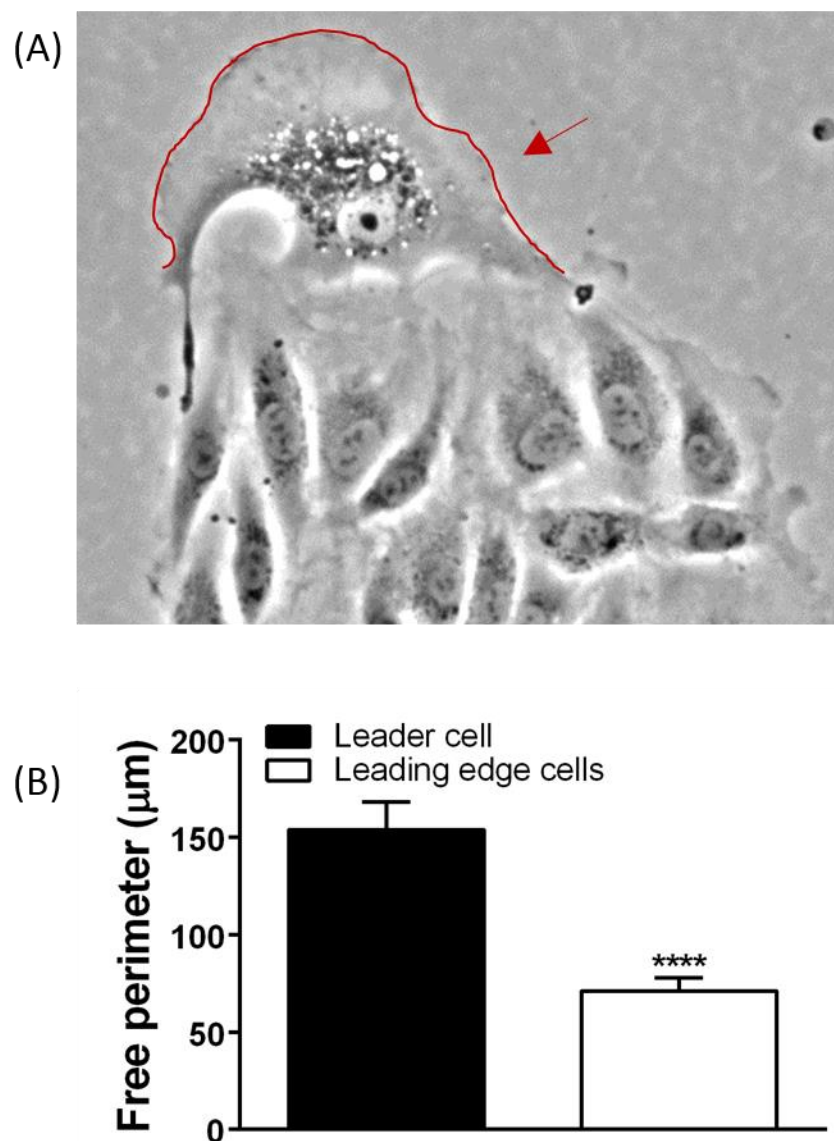


Figure 8. The free perimeter of leader cells is around two folds larger than that of the other cells at the leading edge.

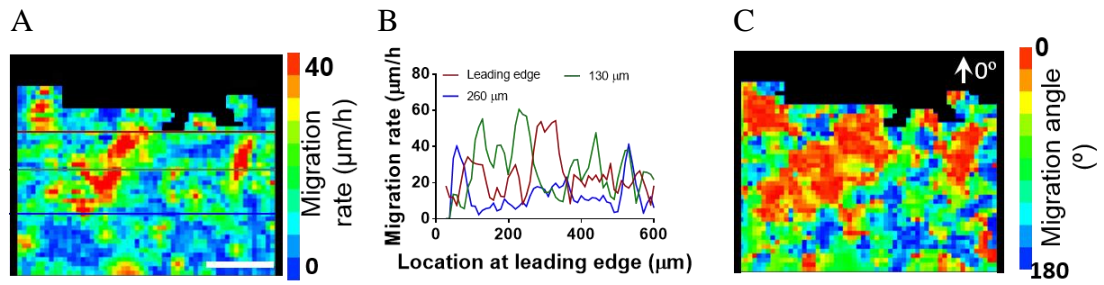


Figure 9. The migration rates at the wound leading edge are unevenly distributed. The distance between the two fast migrating cell groups is in the same level of the distance between two nearby leader cells.

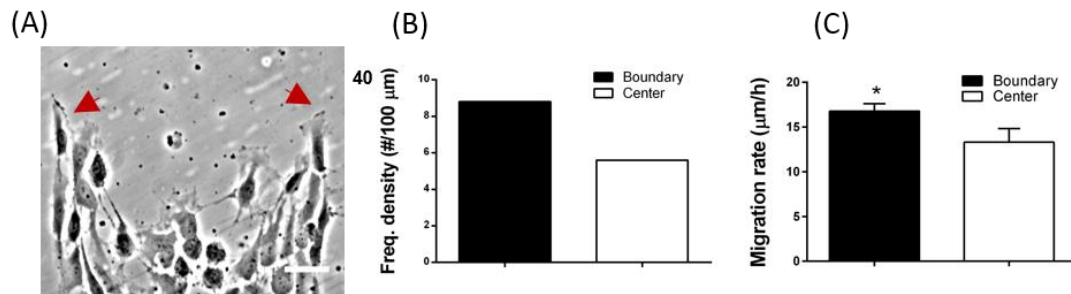


Figure 10. The leader cells maintains a high distribution frequency at the boundary of the rectangular pattern, and the cells at boundary migrate significantly faster than the cells at the center of the cell monolayer. (A) Representative images of the leader cell location; (B) the distribution frequency of the leader cells along the leading edge; (C) the migration rates of the boundary and center region of the leading edge.

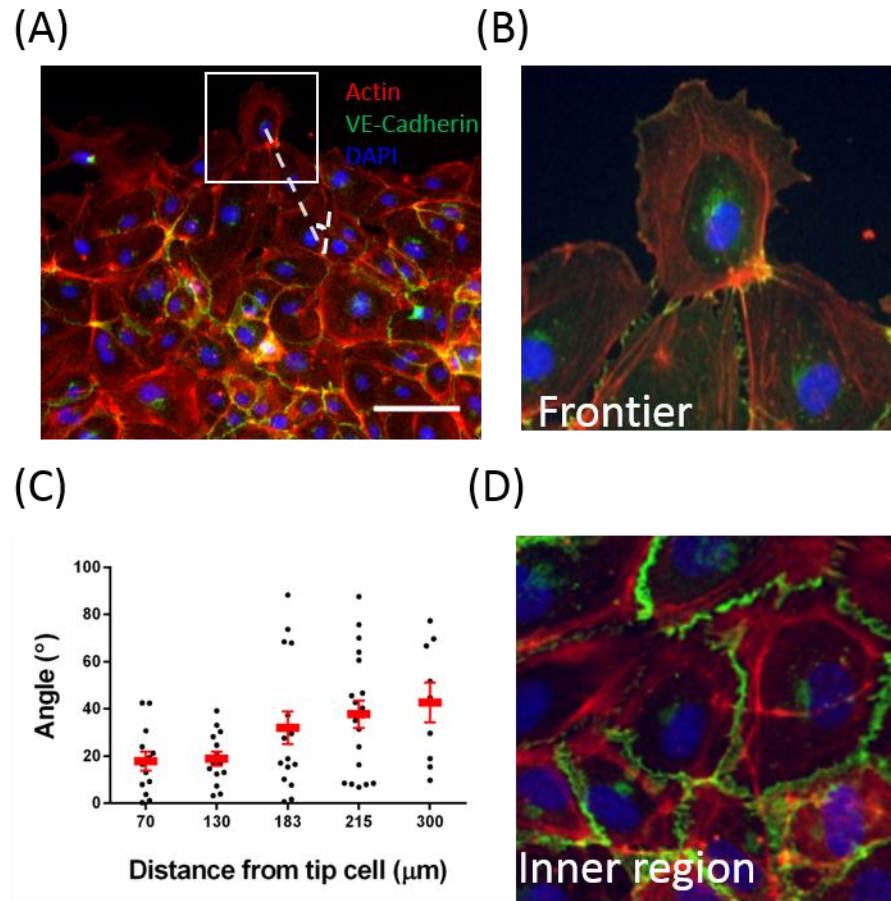


Figure 11. The actin stress fiber in the follower cells are aligned towards their leader cells, and the frontier cells and leader cells have a higher expression level of stress fiber compared with the cells in the inner region of the monolayer. (A) Actin stress fiber distribution within cells in wound healing assay; (B) the stress fiber of leader cells; (C) the alignment of the stress fiber of follower cells to their leader cells; (D) the stress fiber expression in the inner region of monolayer.

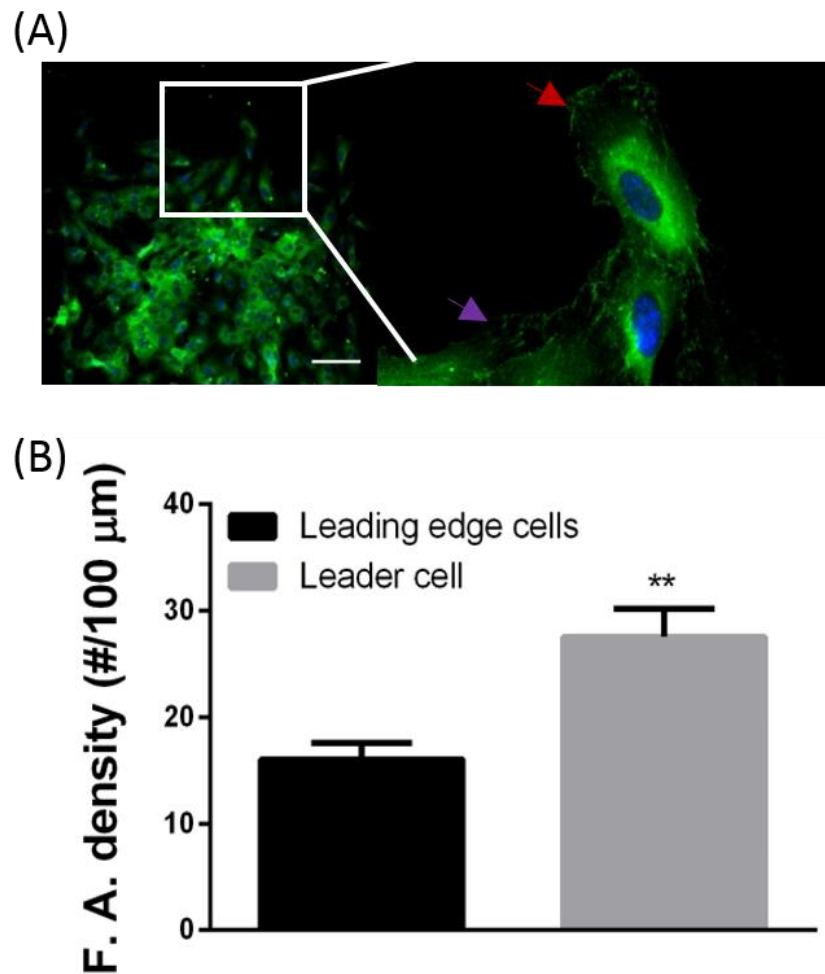


Figure 12. The leader cells maintain a higher density of focal adhesion sites compared with that of the other cells at the wounding frontier. (A) Representative images of the focal adhesion distribution, green: vinculin, blue: nucleus. Scale bar, 50 μm .

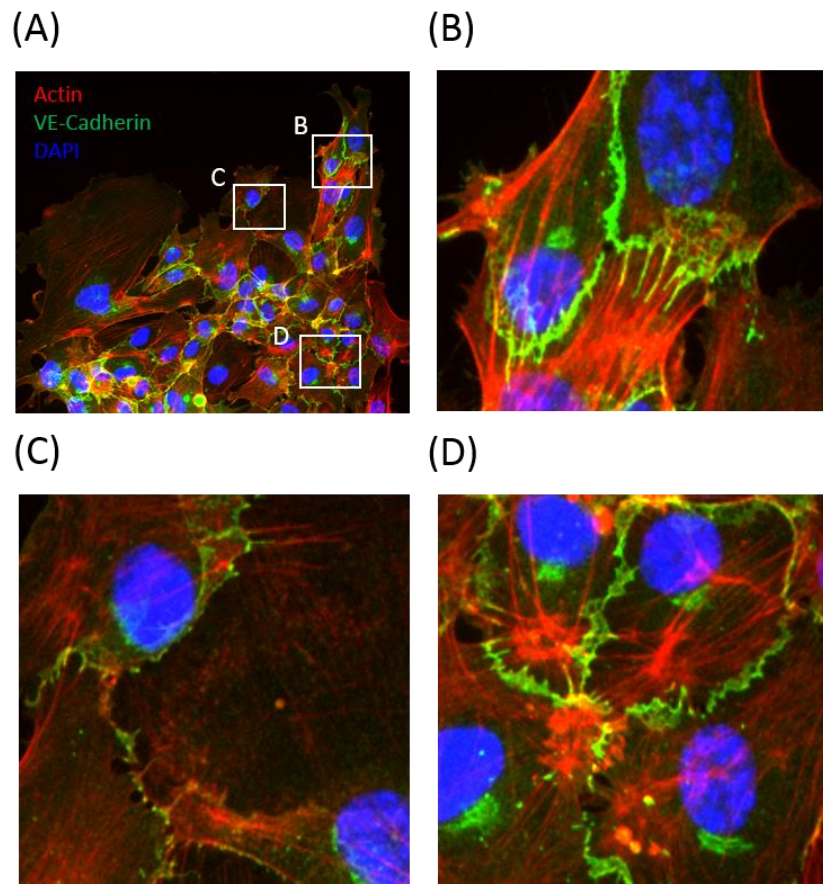


Figure 13. The adhesions junctions form focal adhesion junctions at the leader edge of the wound. (A) The structure of VE-Cadherin and actin stress fiber distribution with in the cell monolayer; (B)-(D) zoomed in images of the adhesions junction structure at the different locations of the monolayer.

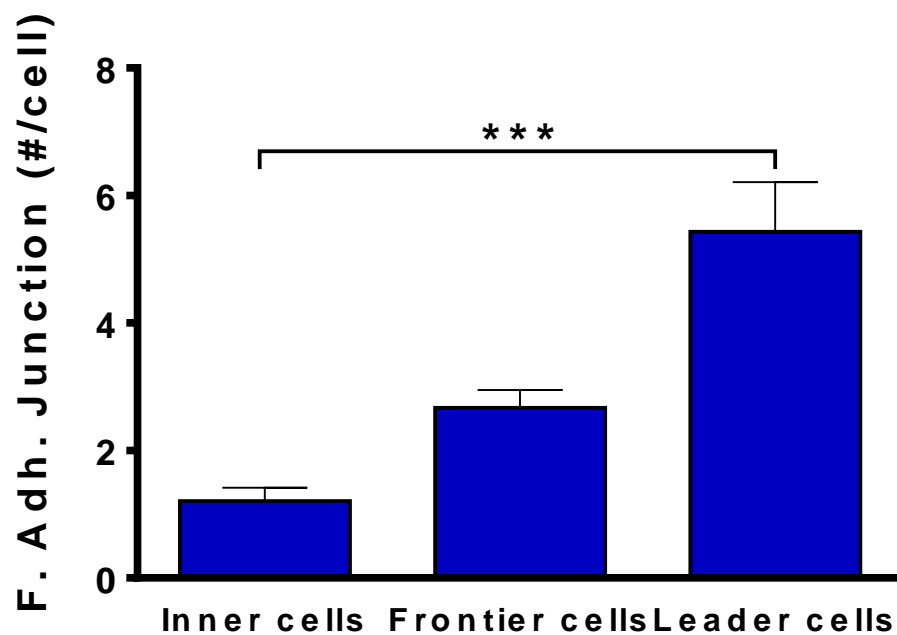


Figure 14. The adhesions junctions form focal adhesion junctions at the leader edge of the wound. (A) the structure of VE-Cadherin and actin stress fiber distribution with in the cell monolayer; (B)-(D) zoomed in images of the adhesions junction structure at the different locations of the monolayer.

4.5 Regulating leader cell density and cell monolayer migration rates via changing geometry of cell monolayer in *in vitro* wound healing assay

To further test our hypothesis that the constant leader cell density is responsible for the constant cell monolayer migration rates in rectangular patterns with various widths, we engineered a method to change the leader cell density, and further test whether this will change the cell monolayer migration rates. The cell monolayer is patterned into trapezoid shape via plasma lithography. By changing the migration direction, either converging or diverging, we can increase or decrease the widths of wound leading edge of cell monolayer (Figure 15 A). After the cell monolayer migrating for 14 to 16 hours, we found that the morphology of the cells at the leading edge dramatically different in cell monolayers with converging, diverging, and rectangular shapes. In converging pattern, the leader cells maintains the motive characters, such as large lamellipodia, during the 14 to 16 hours. As the wound leading edge getting narrower and narrower, the leader cells condensed at the wound leading edge. Thus, the leader cell density increased dramatically, from 6/mm to 10/mm (Figure 16 A). Eventually, the leader cells occupied the whole leading edge and some leader cells lost their direct follower cells (Figure 15 A). In diverging shaped cell

monolayer, as the cell monolayer migrating forward and the leading edge getting wider, new leader cells are formed and the leading edge maintains a constant leader cell density (Figure 15 B). In the rectangular pattern, the leader cell number and density do not change as we observed in the experiment in previous section (Figure 15 C, and Figure 16 A). This method enables us to manipulate the leader cell density without biologically manipulating the cells.

Interestingly, the cell monolayer migration rates during cell monolayer migration vary differently according to the geometry of the cell monolayer. In converging pattern, the cell monolayer migration rate increases as the monolayer migrating forward, while in diverging shaped cell monolayer, monolayer migration rates decreased. Consistent with previous experiments, the leader cell density and cell monolayer migration rates maintains constant in rectangular shaped cell monolayer (Figure 16 B). Comparing the cell monolayer migration rates and leader cell density after cell monolayer migrating for 16 hours, the monolayer migration rates and leader cell density in the converging pattern are significantly higher than those in the diverging and rectangular patterned cell monolayer (Figure 16 C and D). To exclude the area variation issues in the converging and diverging shaped cell monolayers as the cell

monolayer migrating forward, cell migration rates based on variation of area were calculated. The results indicated that the migration rates in cell monolayer with diverging shape maintains constant, and that of the converging cell monolayer increased as shown in the Figure 5 (Figure 17). Comparing the migration rates variation during cell monolayers migration, the acceleration of the converging cell monolayer migration is positive, which indicated that the cell monolayer migration increases as the cell monolayer migrating forward. The acceleration in rectangular shaped cell monolayer maintains around zero, which is consistent with the robust migration rates in this cases. The acceleration in diverging case is averaged as a negative value, which may because of the variation of area per unit advances. Over all, this experiment confirmed that the cell monolayer migration rates can be regulated through changing the leader cell density via control the geometry of the cell monolayer.

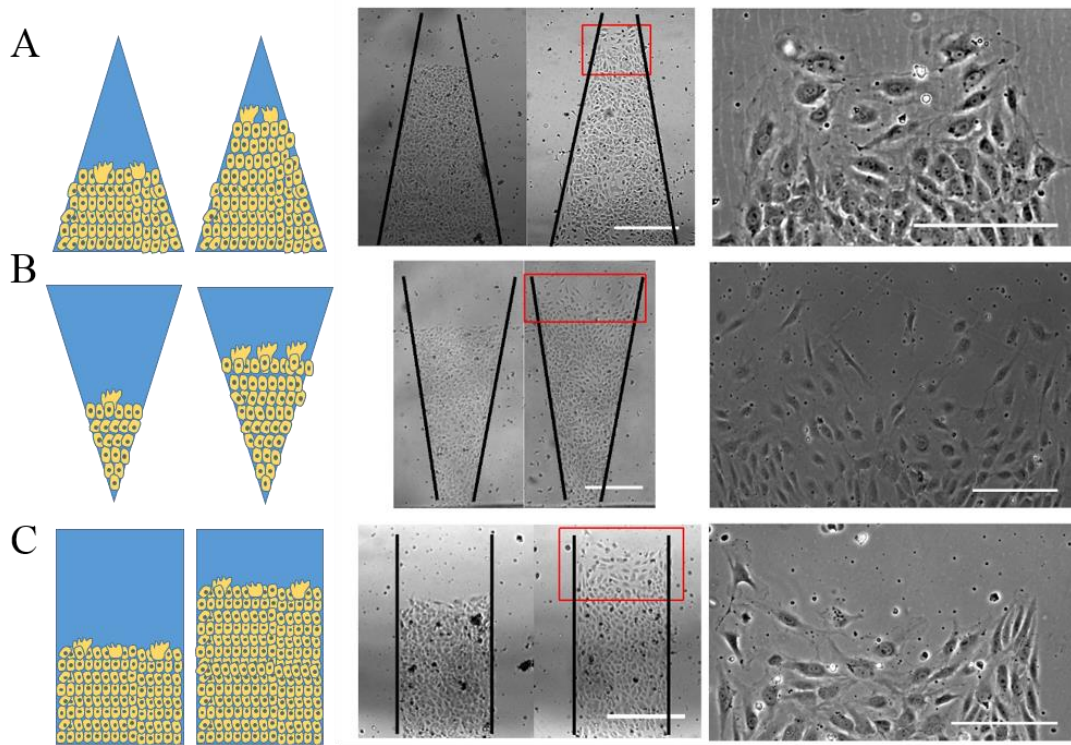


Figure 15. Modulating leader cell density via changing geometry of cell monolayer.

(A) Increasing leader cell density via converging shaped cell monolayer; (B) Increasing leader cell number via diverging shaped cell monolayer; (C) Rectangular shaped cell monolayer maintains constant leader cell number and density.

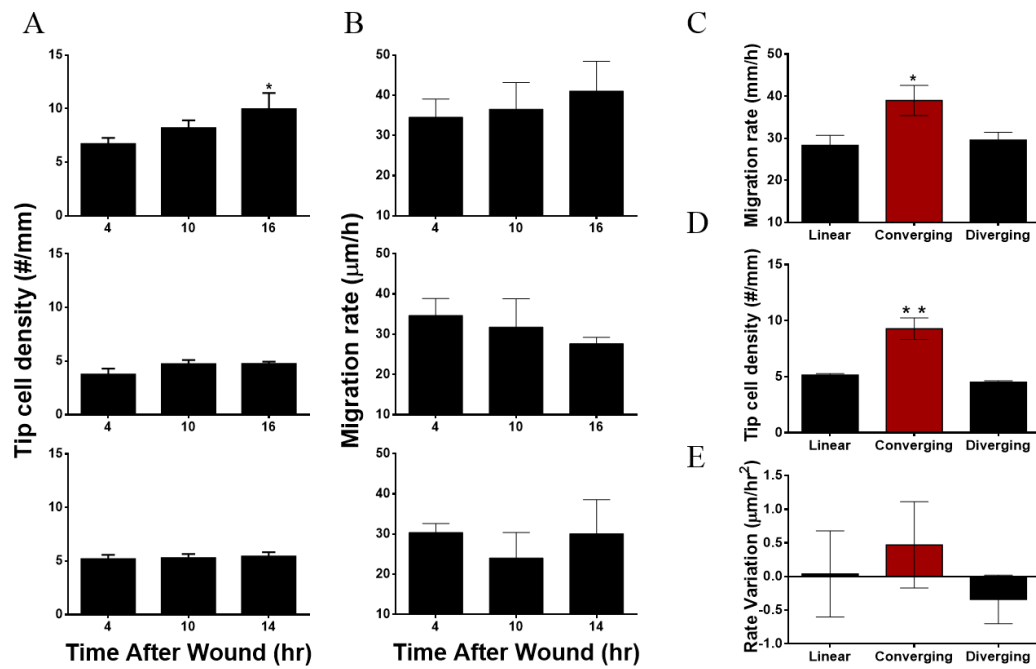


Figure 16. Geometry of cell monolayer and migrating direction modulate leader cell density and monolayer migration rates. (A - B) leader cell density (A) and migration rates (B) variation during collective cell migration in different geometrical cell monolayers; (C – E) Comparing migration rates (C), leader cell density (D), and rate variation (E) 16 hours after wounding in different geometrical cell monolayers.

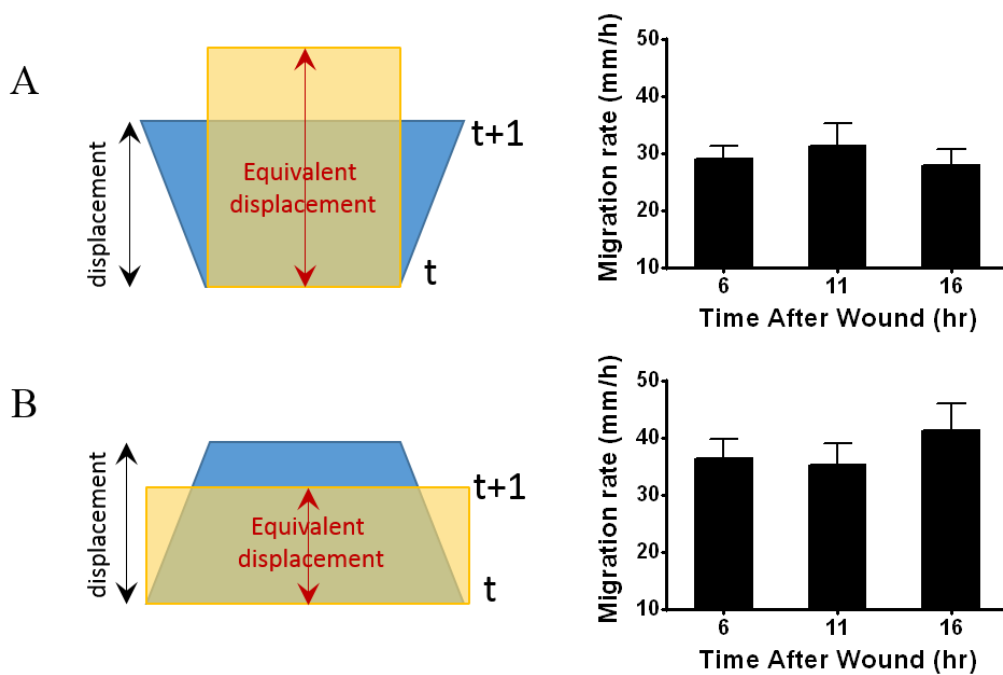


Figure 17. Migration rates calculated using equivalent displacement from area variation in converging (A) and diverging (B) cell monolayer migration;

4.6 Higher leader cell density enhances the correlation level of the cell migration during collective cell migration

Experiments in previous section have shown that the cell monolayer migration rates can be regulated via the manipulating the leader cell density through changing the cell monolayer geometries. To further elucidate the effect of leader cells on cell monolayer kinetics, the velocity of cells was mapped onto the whole monolayer at various time points during collective cell migration via PIV method [6, 79]. Regarding to the instantaneous migration rates, it did not change dramatically in both converging and diverging cases (Figures 18 B, 19 B). This means that the motility of individual cells is not enhanced or diminished. From the spatial distribution of migration rates within the cell monolayer, cell monolayer in both cases maintain an active leading edge region. This indicated that the leading edge cells pulling the cells in the inner region to heal the wound (Figure 18 B, 19 B). In converging cell monolayer, this active region is much longer from the leading edge to the inner region, compared with that in the diverging case. In addition, the angle between the direction of migration velocity and the direction towards the wound leading edge is significantly different in cell migration in converging and diverging patterned cell monolayer (Figure 18C and 19 C). In

converging patterned cell monolayer, the cell monolayer maintains a small angle, around 45 degrees, at the region of 300 micron from the leading edge (Figure 18 C). While in the diverging case, the migration angle is larger compared with the converging case, around 100 degrees. In addition, the angle at different locations within the cell monolayer has no significant differences (Figure 19 C). These data clearly showed that the leader cells guide the cell monolayer migrating forward via changing the migration angle relative to leading edge.

To further comparing the converging and diverging cases directly in the same scenario, a competing wound healing assay was performed. In this experiment, the cell monolayer was also being patterned into trapezoid shape, but being wounded both at the diverging and converging directions. The cell monolayer behavior during collective cell migration was observed and analyzed (Figure 20 A, B). Consistent with results in previous section, the cell monolayer migration rates and leader cells density in converging pattern are larger than those in diverging case (Figure 20 C). By mapping the velocity distribution within the cell monolayer, we analyzed the migration rates and migration angle relative to the direction towards the wound leading edges (Figure 21). Regarding to the cell migration rates within the monolayer, cells at leading edge in both

directions developed an active migrating region. Consistent with the mono direction assay, the active region in the converging direction occupied a longer range from the leading edge to the inner region (Figure 21 C, D). The area migrating to each direction was calculated. The results indicated that the ratio of area towards each direction was 1:1 after 6 hours migrating, this may be because the leading edge width is much narrower in converging direction compared with the diverging direction (Figure 22). The migration angle of the cells in the monolayer is eventually organize towards the leading edge respectively during the cell monolayer migration (Figure 21 A, B). At 1 hour after wounding, the cell motion was almost random in the inner region of the cell monolayer, and the leading edge developed a small region mainly migrating towards the cell-free region. 3.5 hours after wounding, cells at both leading edge developed an active frontier region mainly migrating towards the cell free region. At this time, the depths of active leading edge in both directions, how far this area cover from the leading edge, are in the same level. 6.5 hours after wounding, the depths of active leading edge region in the converging directions is larger compared with the diverging case. The depth is around 500 μm , compared with 200 μm in the diverging case.

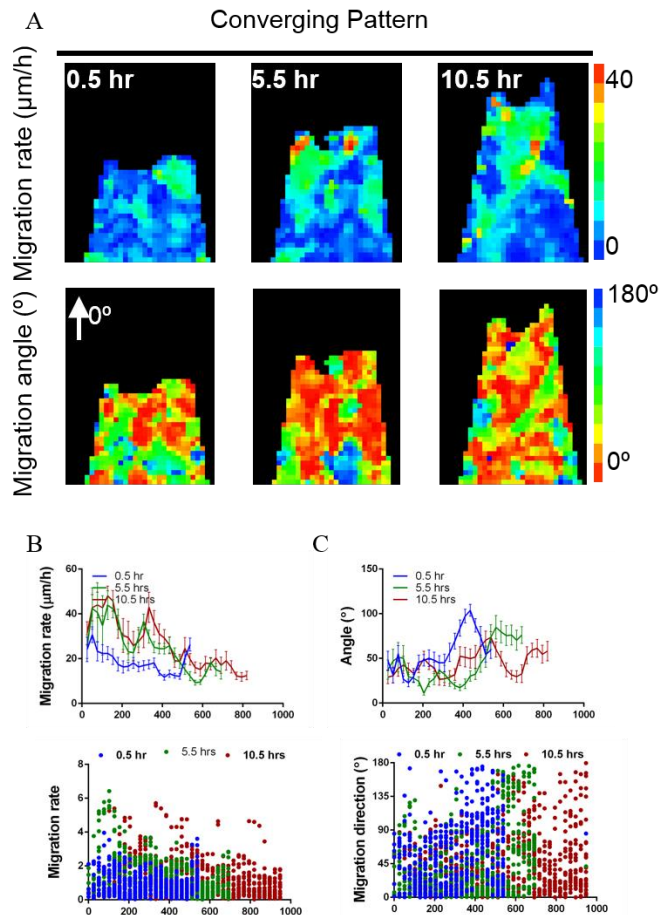


Figure 18. PIV analysis indicates that the cell monolayer migration rates increase as the leader cell density increases. (A) Migration rates and direction distribution within the converging cell monolayer at different time points. (B) The migration rates distribution from the leading edge to the inner region of the monolayer; (C) The migration direction distribution from the leading edge to the inner region of the monolayer.

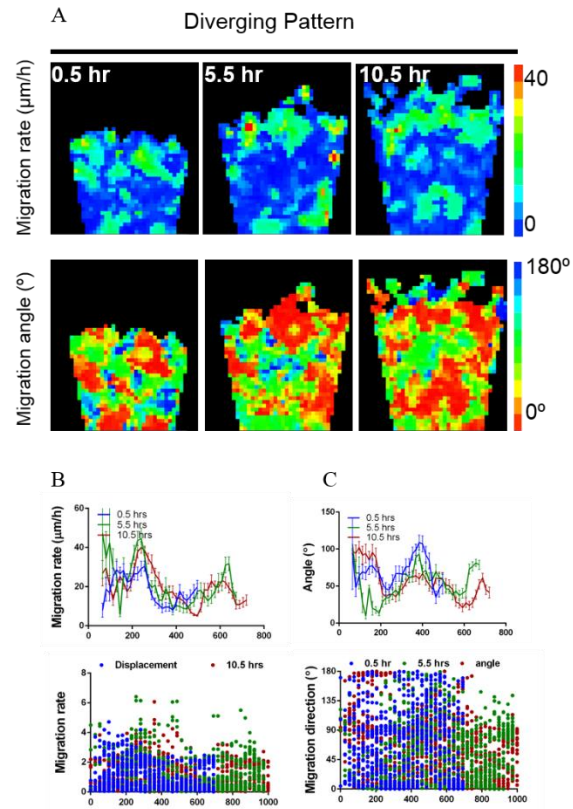


Figure 19. PIV analysis indicates that the cell monolayer migration rates maintain constant in diverging pattern. (A) Migration rates and direction distribution within the diverging cell monolayer at different time points. (unit: $\mu\text{m/hr}$) (B) The migration rates distribution from the leading edge to the inner region of the monolayer; (C) The migration direction distribution from the leading edge to the inner region of the monolayer.

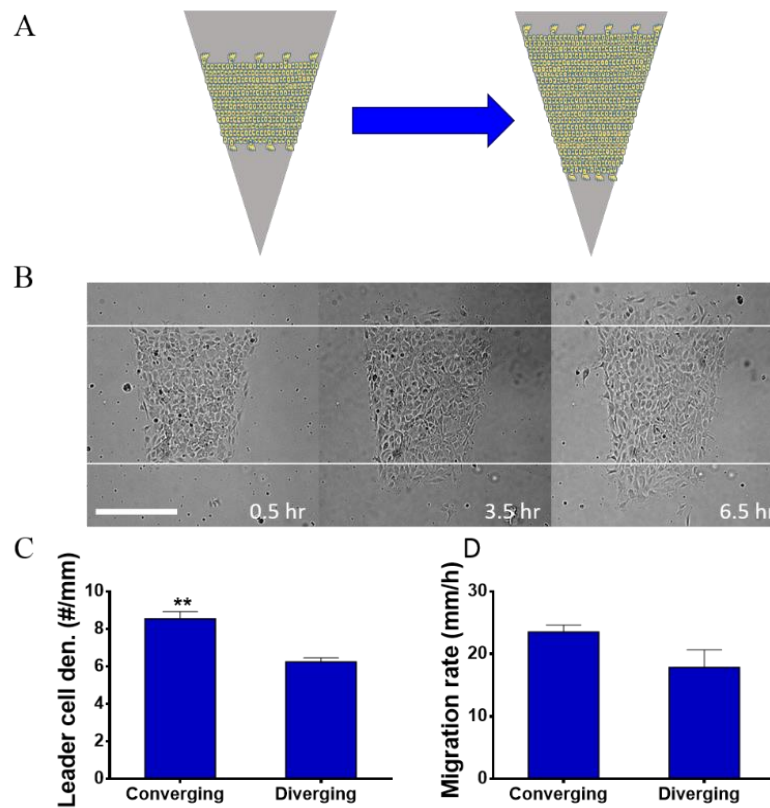


Figure 20. Competing wound healing assay. (A) the concept of competing wound healing assay; (B) Representative images of competing wound healing assay; scale bar, 250 μm ; (C-D) Leader cell density (C) and migration rates (D) in converging and diverging directions in competing wound healing assay.

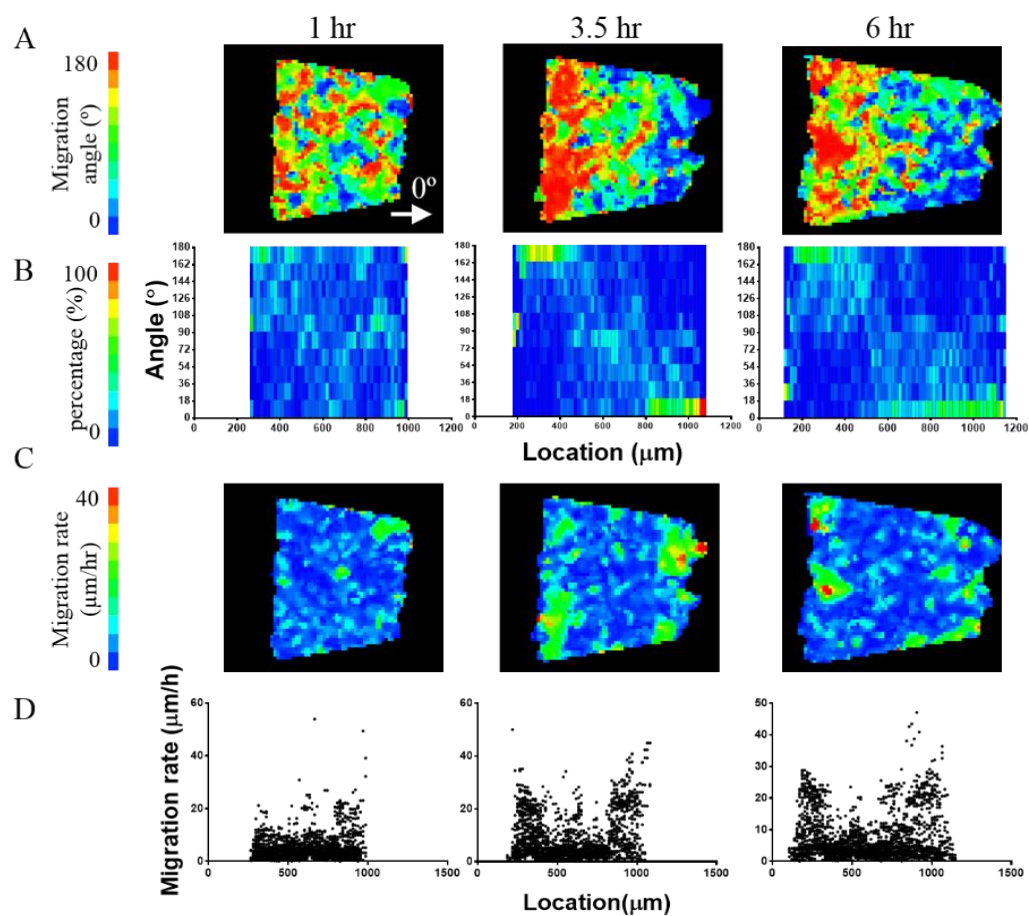


Figure 21. PIV analysis of the competing pattern. (A-B) migration rate and angle mapping on the cell monolayer; (C-D) quantitative analysis of the migration rates and angle distribution in the direction parallel with the wound leading edge.

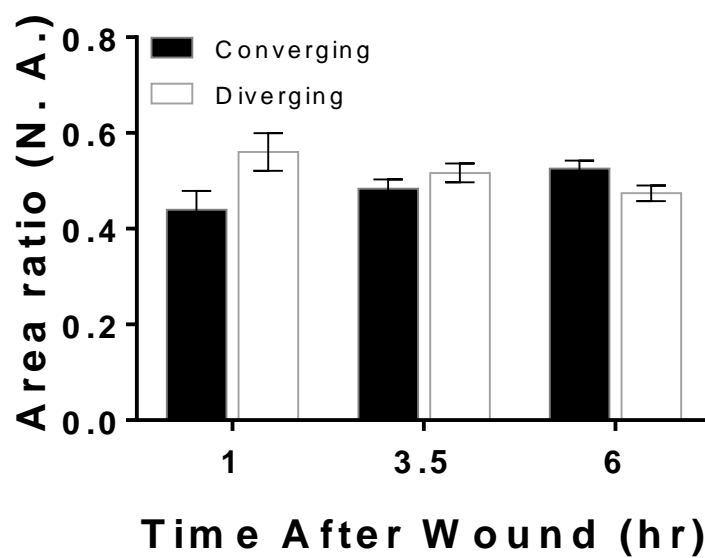


Figure 22 Area percentage of cell monolayer migration toward converging and diverging directions in competing wound healing assay.

4.7 Discussion:

It has been proposed for decades that leader cells are important in collective cell migration [5, 101, 102]. We hypothesized that increasing leader cell numbers will enhance the cell monolayer migration in *in vitro* wound healing assay. The results in this study revealed that it is not the number, but the density of the leader cells affects the cell monolayer migration. We first demonstrated that the leader cell density in *in vitro* wound healing assay maintains constant. We further engineered a method to regulate the leader cell density via modulating the geometry of the cell monolayer. Via this method, we found that cell monolayer migration can be regulated by changing leader cell density during wound healing process.

Leader cell maintains active characters and guides the cell monolayer migration

In endothelial cell monolayer, we observed the leader cells are morphologically distinct from other cells. During angiogenesis, endothelial cells developed tip cell to guide the stalk cells migrating forward [36]. These tip cells maintain extension of long filopodia to facilitate their ability to protrude forwards. This is consistent with the extension of large lamellipodia of leader cells in the endothelial cell monolayer to

facilitate migration. It has been reported that leader cells in collective cancer cell migration also maintain a larger free perimeter [38]. Though the cells at the inner region of the cell monolayer can also develop secret lamellipodia underneath the front cells [37], the other leading edge cells cannot developed this structure towards leading edge since the spatial confinement. Even the secret lamellipodia exists in other leading edge cells, it cannot contribute to migration towards leading edge. From the velocity mapping of rectangular shaped cell monolayer, it is clearly shown that the cell monolayer at leading edge are divided into groups according to the migration directions and rates. The motion of endothelial cell monolayer can form flow pattern, with the width around 100-200 μm [24]. For the cell migration at the wound leading edge, the cells also formed groups around the leader cells with higher migration rates and particularly migrate towards the cell-free region. The distance between neighbor leader cell groups is around 200 μm , which is in the same level of the width of cell motion flow reported in ref. [24]. We found that the boundary of rectangular pattern has a higher probability to locate a leader cell. The corner of rectangular cell monolayer maintains higher mechanical stress compared with that of the inner region [80], and high mechanical stress induces cell branching in 3-D micro-engineered tissue model

[103]. In *in vitro* wound healing assay, mechanical pressure stimulates the formation of leader cells in cancer cell monolayer [38]. In endothelial cell monolayer, the higher mechanical stress may also enhance the formation of leader cells to facilitate the cell migration forward. In endothelial cell, mechanical stress induces the expression of Vascular endothelial growth factor (VEGF) [104, 105], which facilitates the development of tip cells in angiogenesis [36] and leader cells in endothelial cell monolayer [24]. Thus we speculate that the higher mechanical stress at the boundary of the leading edge may enhance the expression of VEGF, and thus induces the leader cells.

The molecular structure of actomyosin, focal adhesion, and adherens junctions also indicates the leader cells guide the follower cells migrating forward. The results indicated that the leader cells express more actin stress fiber compared with the cells in the inner region, which means the leader cells generate larger contraction force [106]. Combined with the high density of focal adhesion sites, the contraction force can be transferred to the cell-substrate interactions, and drive the leader cell itself and its follower cells migrating forwards. The actin stress fiber of follower cells are aligned to their leader cell with a distance related manner, which indicates the interaction of leader

cells and its direct follower cells can be transmitted to further region of the monolayer.

The higher frequency of focal adherens junctions between the leader cells and their follower cells also shows the strong mechanical force between them. The stress fiber at the focal adherens junctions can insert into adherens junctions, rather the focal adhesions, to link the endothelial cell together to transmit mechanical force [106].

Geometrical confinement regulates leader cell density and hence modulates cell monolayer migration

The physical environment affects the cell behavior in collective cell migration in *in vitro* wound healing assay [3, 38, 107, 108]. Specifically, the geometry of the cell or tissue also regulate morphogenesis[103, 109], stem cell differentiation [110]. In addition, the geometry of the cell monolayer can also induce emerging mode of cell migration[79, 111], and affect the leader cell formation[91]. Here, we show that via changing the cell monolayer geometry, the leader cell density can be manipulated, and hence the cell monolayer migration behavior is modulated. Via this method we confirmed a general pattern during collective cell migration: the constant leader cell density is responsible, or partially responsible, for the constant monolayer migration

rates. It has been reported that only the width at the single cell wide level that it affects cell migration rates and mode[79], which is consistent with our rectangular shaped cell monolayer. The leader cell densities are at the same level with rectangular shaped cell monolayers and cell monolayer without geometrical confinement. This indicates that the self-organizing rules of leader cell formation is robust to the width of cell monolayer. In converging shaped cell monolayer, the leader cell density increases due to geometrical confinement. The leader cells are squeezed as the leading edge getting narrower and narrower. These leader cells maintain its motive characters, such as larger lamellipodia structure. Even some leader cells lost direct follower cells, the mechanical force generated by these cells can also transmitted to the cell monolayer layer due to the focal adherens junctions. In diverging pattern, the leader cell density at leading edge maintains constant since the increasing width of leading edge induces more leader cells.

In converging, diverging, and rectangular shaped cell monolayer, the migration rates have the same variation pattern as those of the leader cell density variation. The PIV results indicate that the migration rates in different cases have no significant variation over time. The leader cells do not increases the cell motility. This conclusion

was confirmed by the competing wound healing assay. It has been reported that the cells at the inner region can also generate a large portion of traction force for cell migration[15]. My results here consistent with their conclusion that leader cells do not generate the main traction force to lead the cell monolayer migrating forward.

The velocity direction distribution within cell monolayer reveals the leader cells guide the cell migration directions to regulate the cell monolayer migration. In converging shaped cell monolayer, the area of cell monolayer mainly migrating toward the leading edge increases as the leader cell density increasing. While in diverging case, the migration direction of cells in monolayer do not have a significant variation. As the leader cell density increasing, the correlation level of the active migrating cells is increased, since the leader cells mainly dedicated migrate toward the cell free region. Via the mechanical interaction through the focal adherens junctions, the coordinated migration can be transmitted to the inner region and affect the cell migration direction. With a higher leader cell density, the focal adherens junctions will be strengthen, and will affect a larger area of the cell monolayer. This highly coordinated cell migration enhances the cell monolayer migration rates. This effect is well illustrated in the competing assay. As the cell migrating forward, the migration angle relative to the

leading edge reduced in both directions. After 6 hours, the migration angle of cells 500 μm behind the leading edge in the converging direction are mainly in the $0-18^\circ$; compared with 200 μm in the diverging direction. It has been reported that in collective cell monolayer migration, local cellular migrations follow local orientations of maximal principal stress [16]. I speculate that leader cells regulate follower cells migration according this rules. As the leader cell density increasing, the coordinating ability of leader cell also increases, which enlarge their affecting area.

Here, our research shows the leader cells guide the cell monolayer migration mainly through coordinating the migration direction of cells in the cell monolayer, and higher leader cell density affects larger distance from the leading edge to the inner region. By enhancing this correlation, the cell monolayer migration rates are increased even the motility of cells do not change. This mechanism can explain the robustness of cell monolayer migration rates relative to the widths of rectangular shaped cell monolayer. The emergent leader cells are the results of interaction among cells in the monolayer. The constant leader cell density provide variable for probing the mechanisms governing the self-organization process of forming leader cells. By explaining the reason of this constant leader cell density, we will gain a deeper

understanding of the physical principles of living matters, which may guide the development of tissue engineering, and help to explain other complex cell behaviors.

Chapter 5

ARSENIC TREATMENT ENHANCES KERATINOCYTE MONOLAYER LEADER CELL FORMATION AND MIGRATION DYNAMICS

5.1. Introduction and objective

Arsenic has been identified as one of the first identified, and most potent carcinogens[112, 113]. Arsenic spreads widely around the world, and can easily dissociated into underground water and affect human health through drinking water[114]. Chronically taking in high concentration of arsenic water induces skin, bladder, and lung cancers[115]. Arsenic contaminated ground water threatens millions of people all around the world, from eastern, southeastern, southern Asia to Latin America, America, and Europe. Among all the cancers related with arsenic, skin cancer is the most common one. Skin lesion is an important sign of in taking high concentration arsenic drinking water. The mechanism of arsenic inducing cancer has been studied intensively. Oxidative stress is a widely studied and accepted mechanism of arsenic toxicity [116]. After treating cells with arsenic, the reactive oxidative species

(ROS) are generated, mainly including hydrogen peroxide[117]. Arsenic induced ROS increases the Nrf2 signaling pathway to protect the cell from it. Nrf2, a transcription factor, regulates the various cell protective proteins, such as NQO1 and HO-1 to protect cells from toxicity of arsenic. Arsenic can increase the expression of Nrf2 at transcription and protein level in human keratinocytes, mainly through the regulation of H_2O_2 [118]. The mechanism arsenic activating Nrf2 and its downstream genes differs from that of SF and tBHQ [119]. Arsenic can induces the Nrf2 in continuing manner, rather than a spontaneous manner.

Besides involved in the arsenic effects signaling pathway, Nrf2 is also involved in epithelial cell migration. Collective epithelial cell migration plays an important role in various physiological conditions, such as cancer metastasis, development. The effects of Nrf2 level on collective cell migration is cell line dependent. Nrf2 level is positively related with migration rate of the corneal epithelial cells[120]. In contrast, the other results shown that up regulating Nrf2 level can reduce the cell migration rate for the breast cancer cell monolayer [55, 60, 121]. Treating cell with arsenic can also affects cell migration. Results shown that arsenic treatment reduces the cell migration rate for the H9C2 myoblast cell line by reducing the Tyrosine Phosphorylation of Focal

Adhesion Kinase [45]. Though the high frequency of skin cancer related with arsenic, the effect of arsenic on skin cancer cell still do not clear. Whether the Nrf2 is related with arsenic altered cell migration is poorly studied.

Arsenic effects on cell migration dynamics should be addressed. In the past decade, the biophysics of collective cell migration has been intensively studied. The emergent leader cells, located at the wound frontier in *in vitro* wound healing assay is related with the cell migration[122] [123, 124]. Mechanical pressure on cell monolayer induces more leader cell and drive the cells toward invasive phenotype [125]. My research on the leader cell concept in the last chapter indicates that leader cell density is positively related with cell monolayer migration rate. Due to the importance of ROS in cell migration, we hypothesized that the arsenic treatment may affect the biophysics of epithelial cell monolayer migration with involvement of Nrf2 signaling pathway. The emergent leader cells' density or phenotype might be altered by arsenic treatment. In this paper, we aims to elucidate the relationship between the arsenic treatment and keratinocyte monolayer migration dynamics, and the role of Nrf2 signaling pathway in this process.

Results

We studied how arsenic affects collective migration of keratinocyte cell (HaCaT) monolayer through *in vitro* wound healing assay. By generating the cell free region by scratch or PDMS blocker assay mentioned in the Chapter 3, the cells migrate collectively to healing the gap. The process of cell monolayer “healing” the wound is observed and analyzed. A representative time sequence image is presented in Figure 23. It shows that arsenic increases the cell migration rate of the cell monolayer.

5.2 Arsenic affects collective cell migration rate with a dose dependent manner

After treating the HaCaT cell monolayer with various concentrations of arsenic for 24 hours, the cell monolayers were wounded to measure the cell monolayer dynamics. The migration rates are strongly related with arsenic concentration. The cell monolayer migrates faster at low concentration (2 μM), and migrates slower at high concentration (10 μM) (Figure 23 B). Particle image velocimetry (PIV) analysis was used to identify the instant migration velocity distribution within the monolayer.

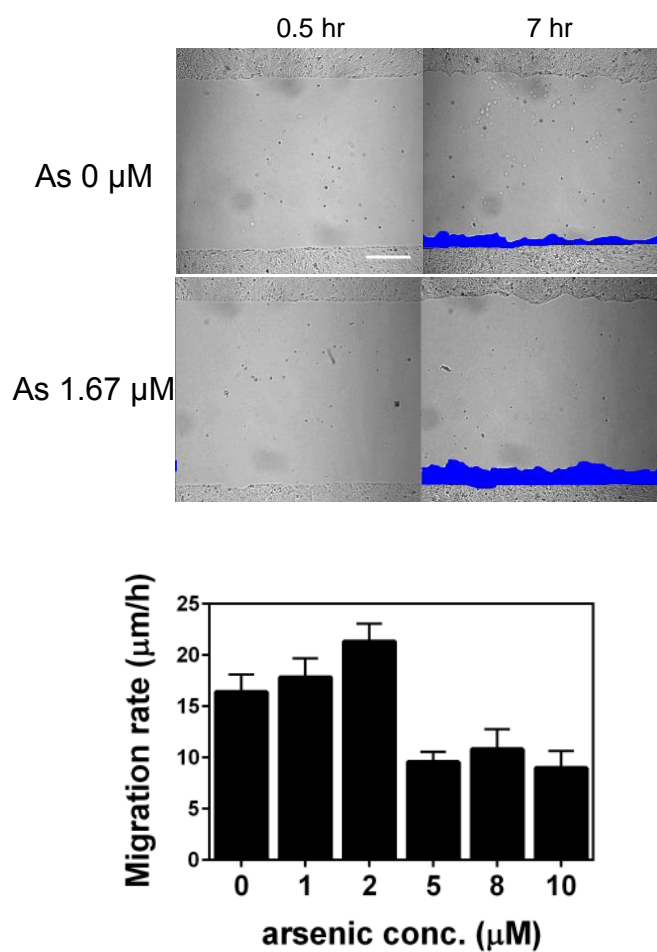


Figure 23. Arsenic treatment increases the cell monolayer migration rates. (A) Representative images for the cell monolayer migration in arsenic treatment and control cases; (B) Low concentration of arsenic treatment increases the cell monolayer migration rate.

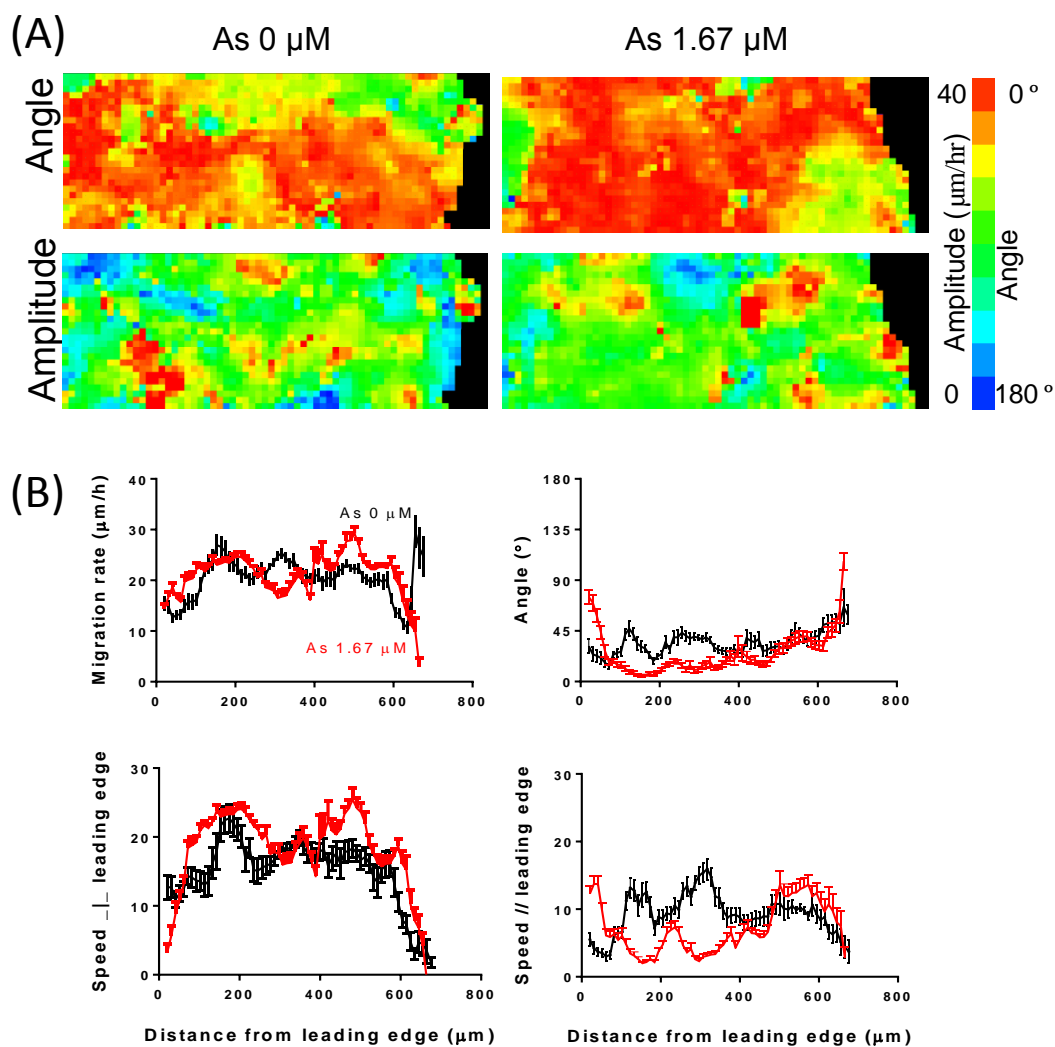


Figure 24. PIV analysis results indicate that arsenic treatment increases the cell migration rates towards the wound leading edge. (A) Representative images for the cell monolayer migration in arsenic treatment and control cases; (B) Migration rates and angle distribution within the cell monolayer.

Consistent with the cell monolayer migration rates results, arsenic treatment increases the cell monolayer migration at the single cell level. Interestingly, the migration rate variation due to arsenic treatment is directional. The migration rates parallel to the wounding frontier maintains at the same level (Figure 24 B). In contrast, the migration rate towards the wounding frontier changes dramatically and maintained the same pattern as the amplitudes of the migration rates. The velocity distribution also varies according to the variation of arsenic concentration. Without arsenic treatment, the cell migration rates distributed evenly in the monolayer. In the contrast, with low concentration of arsenic the cells at the wound frontier moves faster 6 hours after the wounding (Figure 25). From the above results, the correlation level of cell monolayer migration has been enhanced. To test this, we calculated the correlation level of the cells at different location in the monolayer with the cells at the wound frontier. The results indicates that arsenic treatment increase the correlation level in *in vitro* wound healing assay with various distances from the wound frontier (Figure 26). Arsenic affects the cell behavior at the single cell level. This collective phenomenon might be induced by the wounding information. The information of free space at the wound

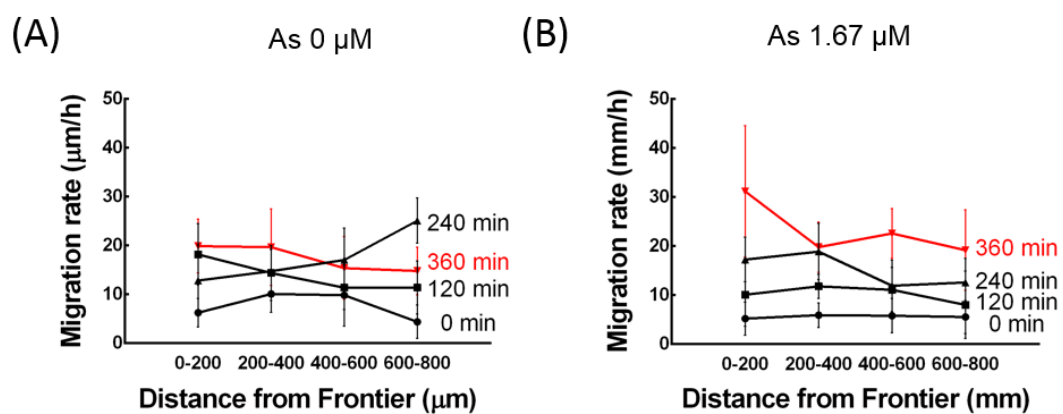


Figure 25. The low concentration Arsenic treated cell monolayer developed a fast migrating leading edge compared with that of the control case.

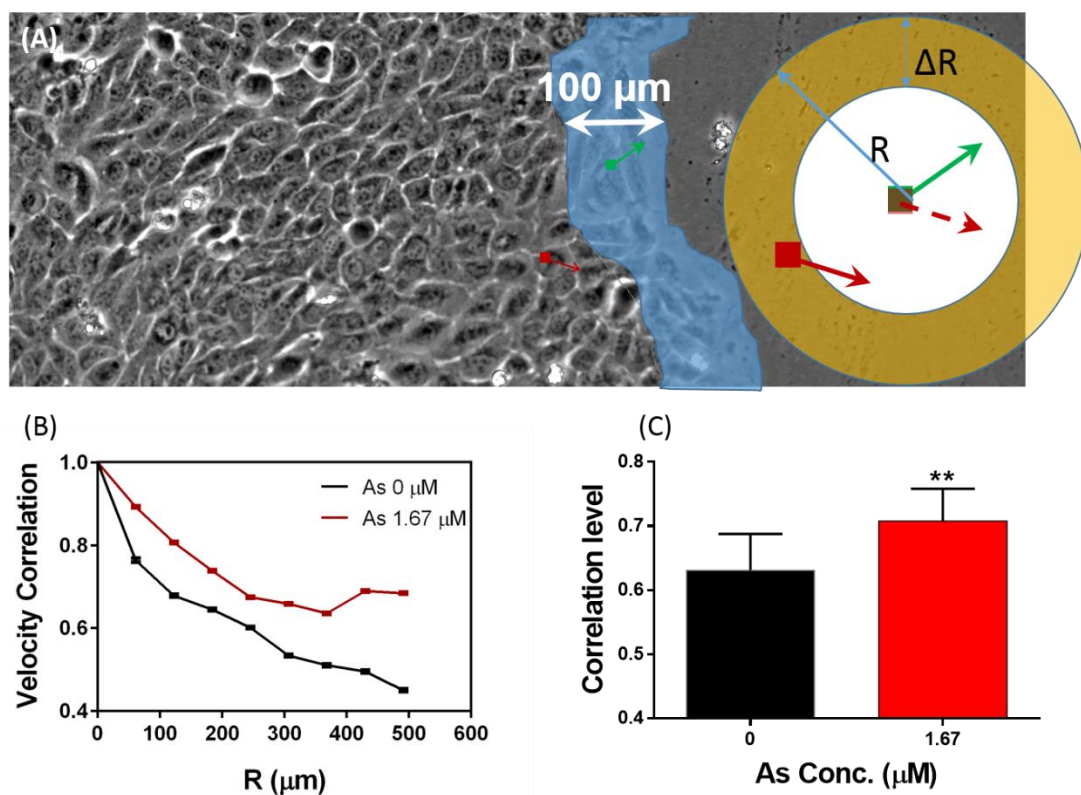


Figure 26. Arsenic treatment increases the correlation level of cell monolayer migration. (A) the concept of correlation level; (B) correlation level of the control and arsenic treated case with the increasing the distance from the leading edge; (C) The correlation level in arsenic treated and control cell monolayer migration.

frontier distributed in the monolayer and induces the migration direction bias towards the wound frontier. We then measured the migration rates and correlation level of cell motion within an integrated cell monolayer. The results indicate that arsenic treatment can increase the motility of the cells and correlation of the cell monolayer migration. The cells are more active after arsenic treatment. In the migration direction, the cells are more correlated after arsenic treatment, while no directional bias was observed (Figure 27). Combined the *in vitro* wound healing assay, these results indicates that arsenic treatment increases the cell motility and correlation level of cell monolayer migration. The wounding generates the migration directional bias.

5.3 Proliferation induced by arsenic do not contribute on its effects on collective cell migration

Arsenic treatment can proliferate the cell monolayer (Figure 28), as the results of cell proliferation assay indicated. It has been reported that cell density within the cell monolayer affected the collective cell migration [126]. To test the contribution of proliferation of cells after arsenic treatment, the cells are seeded to form an integrated

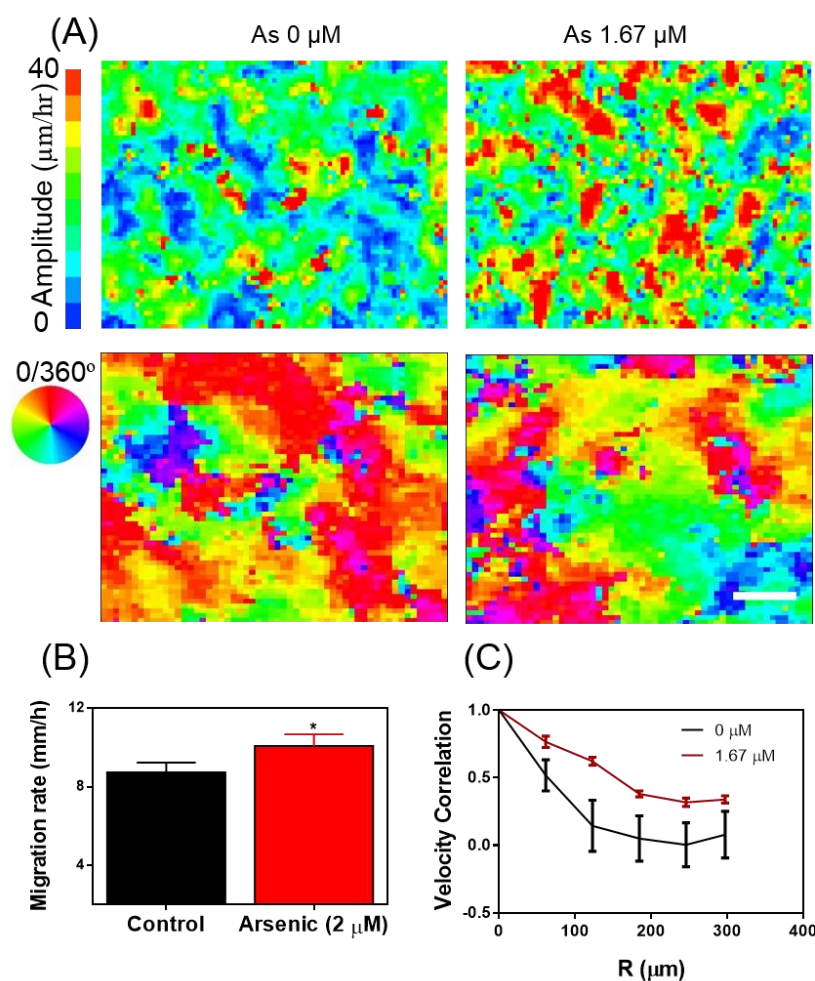


Figure 27. Arsenic treatment increases the correlation level and motility of integrated cell monolayer. (A) The migration direction and amplitude distribution within an integrated cell monolayer; (B) The migration rates in arsenic treated cell monolayer and control case; (C) correlation level of the arsenic treated cell monolayer and control case.

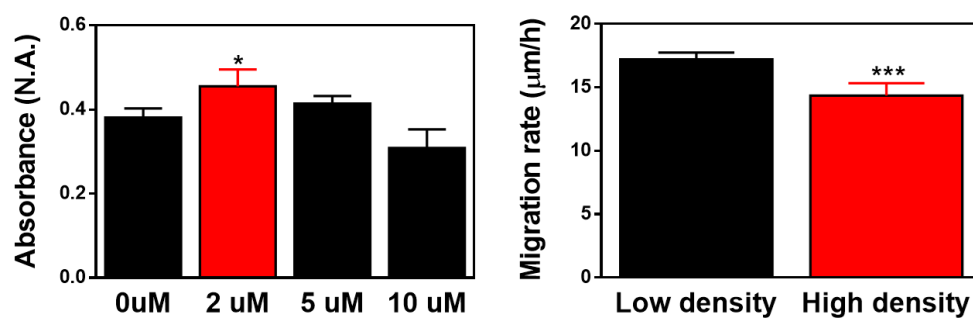


Figure 28. The proliferation effects on HaCaT cell monolayer reduces arsenic effects on cell monolayer migration. (A) Low dose arsenic treatment proliferates HaCaT cell monolayer; (B) the cell monolayer with high cell density migrates slow compared with that of the cell monolayer with low cell density.

cell monolayer with high and low cell density, and the cell migration during the wound healing process was observed. The migration experiment shown that high cell density can reduce HaCaT cell migration (Figure 28). This means that proliferation effects of arsenic treatment reduces its effect on cell migration of arsenic.

5.4 Arsenic affect the phenotype of the emergent leader cells

Cells at the wound frontier do not migrate evenly. The straight linear wound frontier forms emergent leader cells, which make the wound frontier more like a curve. Leader cells guide the cell monolayer migrates into the cell free region. The leader cells maintain a large lamellipodium and more spread out compared with other cells at the frontier or the inner monolayer (Figure 29). At low concentration of arsenic, the leader cells are larger and maintains longer free boundary. They have more focal adhesion sites according to the staining of vinculin. In the contrast, the high concentration of arsenic treatment reduces the number of focal adhesion sites. The leader cell density changes dramatically with low concentration of arsenic. The leader cell density almost doubled in 2 μM arsenic treatment. This makes the frontier curvature index is much larger than that of the control. The protrusion leader size and the advances of leader

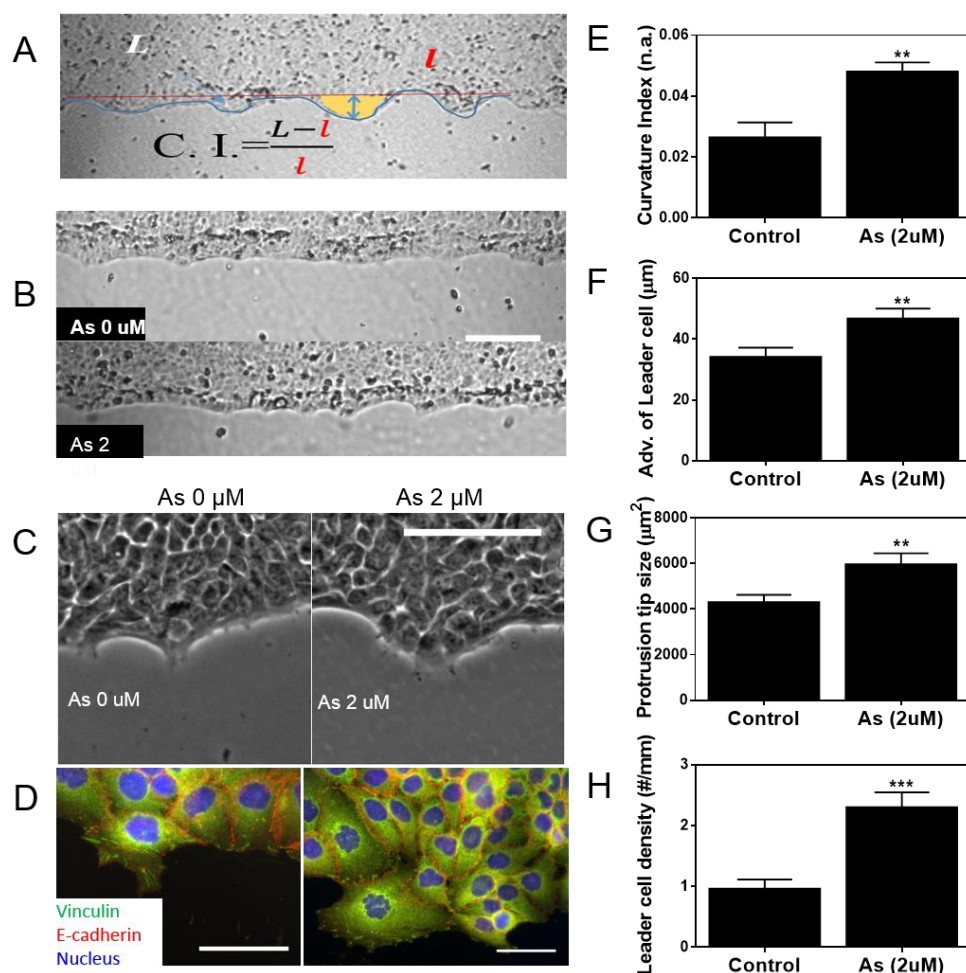


Figure 29. Arsenic treatment enhances the leader cell characters to driving the cell monolayer migrating forwards. (A) concepts of parameters used to characterize the leader cells; C. I., curvature index, L , contour length of wound leading edge, l , linear length of wound leading edge; (B-D) representative images of leader cells in control and low dose arsenic treatment cases; (E-H) leader cell characters in arsenic treated and control cases. Scale bar (B, C) 250 μ m, (D) 50 μ m.

cell is the same as those in the control experiment.

5.5 Arsenic modulates actin stress fiber and focal adhesion sites

To measure the arsenic effects on the expression level of cell motility related proteins, immunofluorescence staining experiments were performed. Arsenic modulates actin stress fiber and focal adhesion sites. The PIV analysis indicates that arsenic treatment increases the motility of single cells within the monolayer. The cytoskeleton protein, actin stress fiber plays an important role in generating contractile force [127]. We hypothesized that arsenic treatment may increase the cell monolayer migration through enhancing the contraction force of each individual cells. The immunofluorescence results indicated that, low concentration of arsenic treatment increases the stress fiber expression level for cells in the monolayer (Figure 30). To generating traction force for cell migration, the cell-substrate interaction also plays an important role from physical perspective. Focal adhesion links the cell with substrate mechanically and chemically. By staining vinculin, a protein involved in focal adhesion, we can exam the strength of the cell-substrate interactions. The results indicates that arsenic treatment alters the distribution of focal adhesion sites at the

wound frontier. After arsenic treatment, the focal adhesion sites are more located at the protrusion leaders at the frontier (Figure 31). This means that the arsenic treated cell monolayer can generate stronger protrusion leader cells.

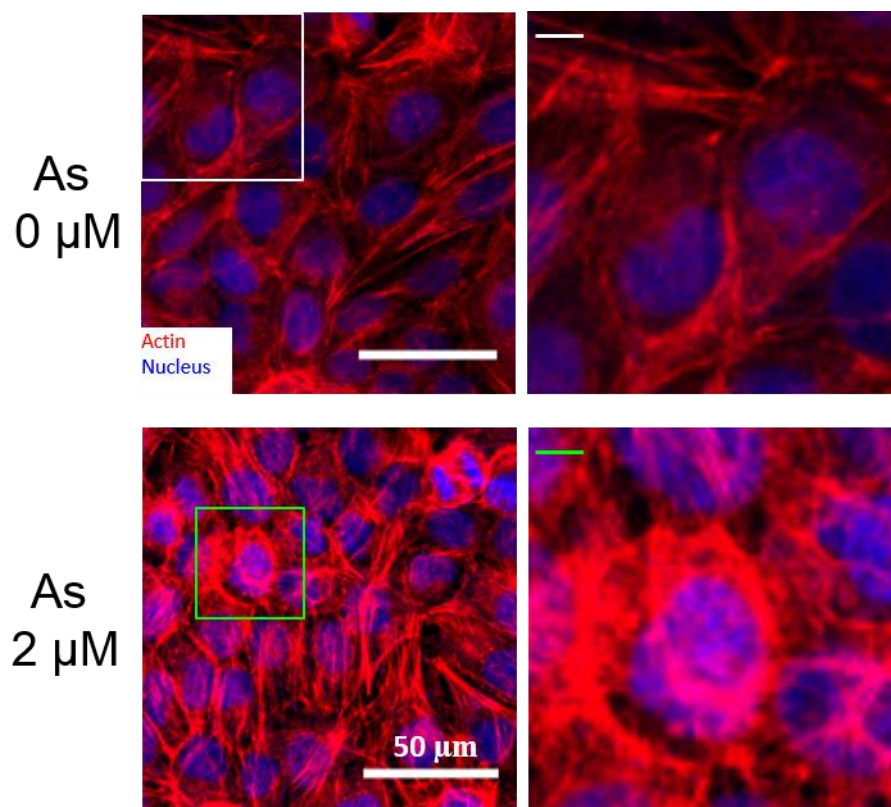


Figure 30. Arsenic treatment increases the expression level of stress fiber.

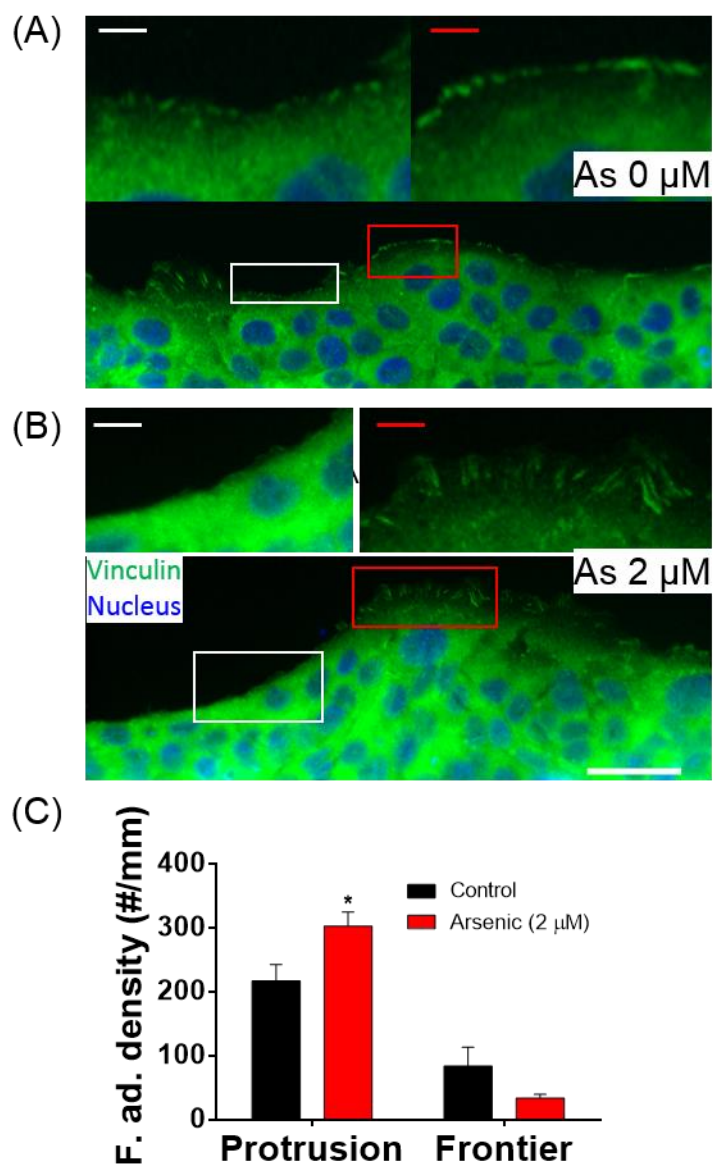


Figure 31. Arsenic treatment condenses the focal adhesion sites at the protrusion leader cells. (A-B) representative images of vinculin distribution within cells, scale bar 50 μm; (C) quantitative analysis of focal adhesion density at Protrusion tips and frontier of the cell monolayer.

5.6 Arsenic modulates E-Cadherin to change the cell correlation level.

The cells within the cell epithelial monolayer are mainly connected through Cadherin enabled adherens junctions. Cadherin, a trans-membrane protein, linked the neighbor cells together mechanically and chemically.

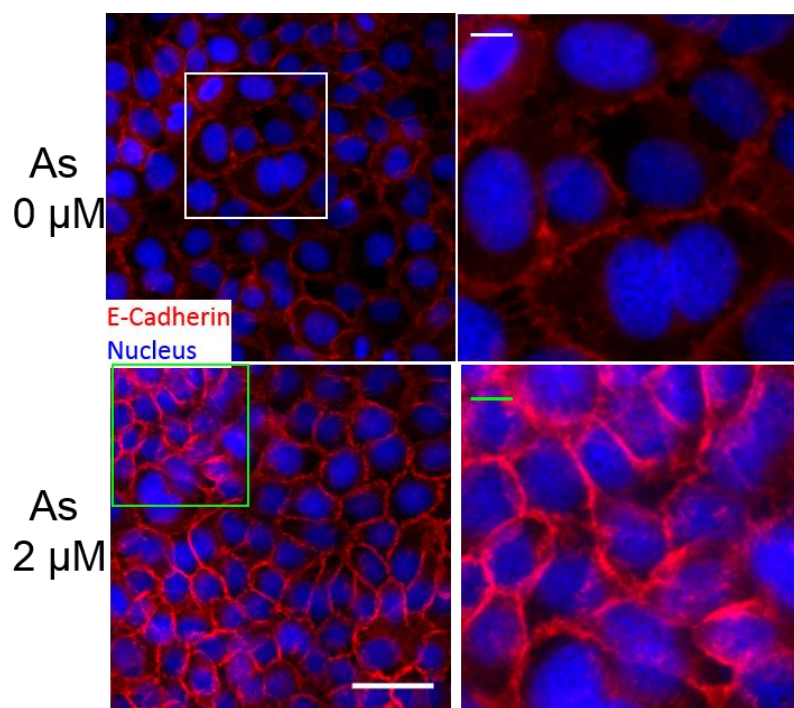


Figure 32. Arsenic treatment increases the expression level of E-Cadherin on the cellular boundary.

The correlation level of Arsenic treatment is related with the E-Cadherin level of the cells. E- Cadherin is the main player in cell-cell interactions. The increased level of correlation make us hypothesize that the expression level of E- Cadherin also increase. By staining the E-Cadherin protein, we confirmed that arsenic can increase the expression level of E-Cadherin, and thus enhances the cell-cell adhesions junctions (Figure 32). We further used western blot technique to probe the E-Cadherin expression with arsenic treatment. The result demonstrates the whole expression level of E-Cadherin does not change (Figure 33). I speculate that arsenic may affect the E-Cadherin involving in the adhesions junctions rather whole cellular expression level.

5.7 Nrf2 signaling pathway involves arsenic enhanced cell monolayer migration.

It has been reported in literatures that the toxicity of arsenic mainly contributed by its induced increasing ROS level within the cell [128]. Nrf2 signaling pathway is plays a central role in protecting the cells from oxidative stress. It has been widely accepted that arsenic treatment induces the expression level Nrf2, both at gene and protein level [51, 53]. To confirm this phenomenon in keratinocyte, we performed

western blot experiments. As shown in Figure 33, arsenic treatment increases the expression level of Nrf2.

To test the Nrf2 signaling pathway is involved in the effect of arsenic on collective cell migration, siRNA gene silencing technique was used to regulate the

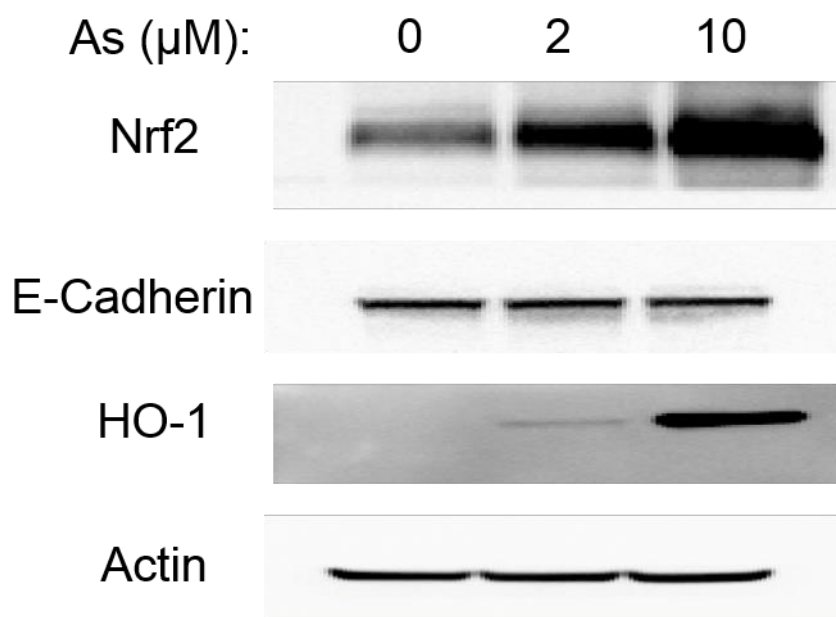


Figure 33. Arsenic treatment increases Nrf2 and its downstream gene, HO-1, expression in a dose dependent manner. The cellular expression of E-Cadherin is not affected by arsenic treatment.

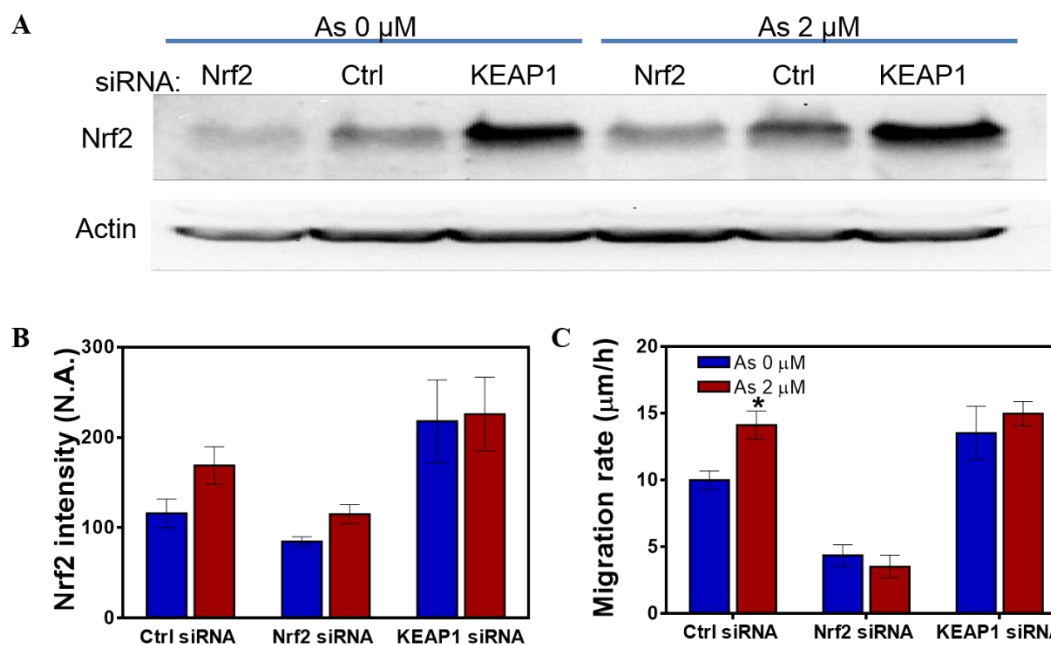


Figure 34. Western blot results indicate that Arsenic increases the Nrf2 expression level at protein level. (A). the effects of arsenic on HaCaT cells with different expression level of Nrf2; (B) the ability of arsenic regulate expression of Nrf2 varies in different Nrf2 expression level; (C) the ability of arsenic regulate monolayer migration varies in different Nrf2 expression level.

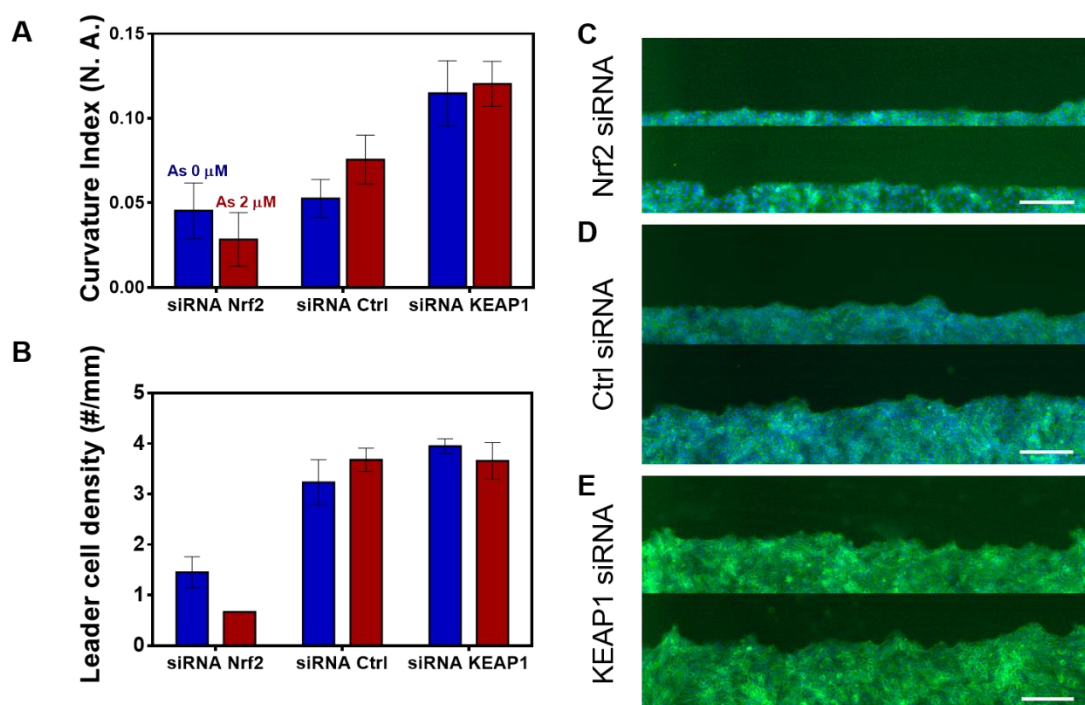


Figure 35. Nrf2 expression level regulates the effect of arsenic treatment on leader cells.

(A – B) arsenic regulation ability on curvature index (A) and leader cell density (B) in different Nrf2 expression level. (C - E) representative images of arsenic treatment under different Nrf2 expression level, scale bar 500 μ m.

expression level of Nrf2 within the cells. Nrf2 or KEAP1 siRNAs were used to down regulate, or up regulate, the Nrf2 expression level. After the gene silencing, the cells were treated with 2 μ M arsenic. The results indicated that the siRNAs gene silencing was effective, and the expression level of Nrf2 are different in these three siRNA cases. In addition Nrf2 expression level in all three siRNA cases with arsenic are higher compared without arsenic treatment case. Further, by measuring the cell monolayer migration rates under three siRNAs, siRNA Nrf2, siRNA control, siRNA KEAP1, the effects of Nrf2 on cell monolayer migration and its role in arsenic effects on cell monolayer migration can be studied. From the arsenic control cases, the results shown that cell monolayer migration rates are positively related with the Nrf2 expression level. Taking the arsenic treatment under consideration, the behavior of cells under these three siRNA are different. The cell monolayer migration only increased in the control siRNA case. Under higher expression level and low expression level of Nrf2, the effects of arsenic on collective cell migration is not significant. In addition, the ability of arsenic regulating Nrf2 expression level was attenuated both in siRNA Nrf2 and KEAP1 treated cell monolayers.

Nrf2 signaling pathway itself regulates the leader cell phenotype. Curvature index and leader cell density increase as the increasing of Nrf2 expression level (Figure 35 A and C). In low Nrf2 expression level case, the leader cell density reduced, while it increases with high expression level of Nrf2 cell monolayer.

5.8 Nrf2 signaling pathway affect the cell migration correlation level.

Previous results indicates that Nrf2 expression level affects the cell monolayer migration rates. To measuring the movement of cells within the monolayer, live cell imaging and PIV analysis was performed. It is clearly shown in the results that cell monolayer with high expression level of Nrf2 migrating much faster compared with the case of low expression level of Nrf2. The same as the modulating Nrf2 through arsenic, the speed parallel with the wounding frontier are at the same level, and the correlation level of the high Nrf2 case are higher than low Nrf2 case (Figure 36). In addition, the Nrf2 expression level also affects the correlation of cell monolayer migration (Figure 37).

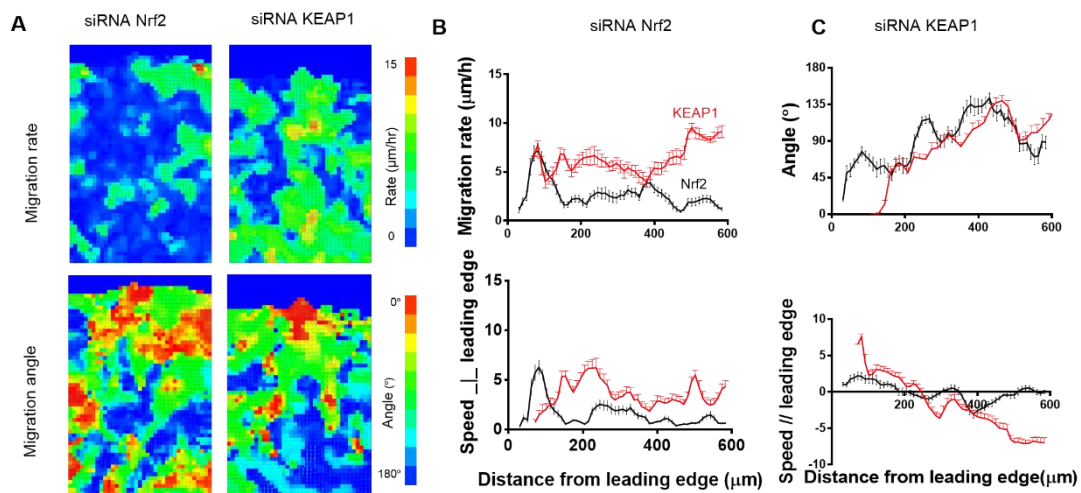


Figure 36. PIV analysis of cell monolayer migration with high and low level of Nrf2 expression. (A). migration rates and migration angle mapping on cell monolayer; (B) quantitative analysis of migration rates distribution within cell monolayer; (C) quantitative analysis of migration direction distribution within cell monolayer.

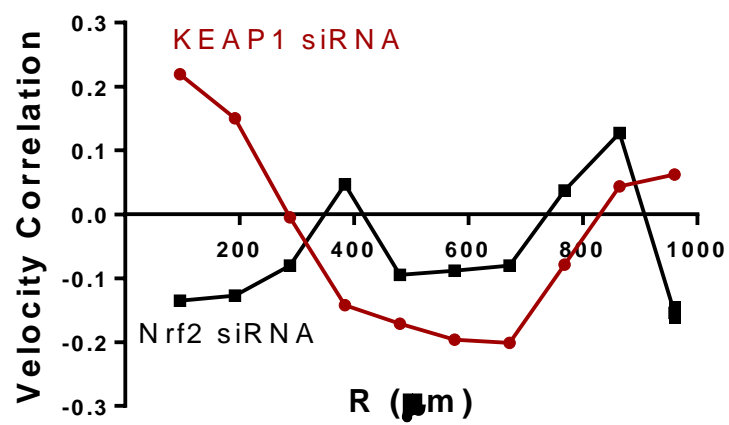


Figure 37. Over expression of Nrf2 increases the correlation level of cell monolayer migration.

Chapter 6

CONCLUSION

The investigation presented herein provides new insights for the function of emergent leader cells in plasma lithography enhanced wound healing assay. We engineered a method to control the geometry of cell monolayer. The correlation of leader cells and cell monolayer migration has been studied via this method. Our results indicated that density of leader cells were quite robust to the width of the cell monolayer in rectangular geometry, and non-patterned cell monolayer. Further the leader cells are characterized from molecular, morphological, and migration dynamical perspective. Our results also indicated the direct correlation of density of leader cells and the cell monolayer migration rates. Our study on arsenic effects on keratinocyte monolayer migration further link our findings with clinical significance. The results indicated that arsenic treatment affects the cell monolayer migration involving Nrf2 signaling pathway. The effects of arsenic on collective cell migration can be explained by the ability of arsenic modulating the leader cells phenotype via regulating the expression

level of Nrf2. As a summary, these study on collective cell migration illustrates the function and importance of emergent leader cells.

REFERENCES

- [1] P. Rorth, "Collective Cell Migration," *Annual Review of Cell and Developmental Biology*, vol. 25, pp. 407-429, 2009.
- [2] P. Friedl and D. Gilmour, "Collective cell migration in morphogenesis, regeneration and cancer," *Nature Reviews Molecular Cell Biology*, vol. 10, pp. 445-457, 2009.
- [3] M. R. Ng, A. Besser, G. Danuser, and J. S. Brugge, "Substrate stiffness regulates cadherin-dependent collective migration through myosin-II contractility," *The Journal of Cell Biology*, vol. 199, pp. 545-563, October 29, 2012 2012.
- [4] G. Fenteany, P. A. Janmey, and T. P. Stossel, "Signaling pathways and cell mechanics involved in wound closure by epithelial cell sheets," *Current biology : CB*, vol. 10, pp. 831-838, 2000-07-15 2000.
- [5] T. Omelchenko, J. M. Vasiliev, I. M. Gelfand, H. H. Feder, and E. M. Bonder, "Rho-dependent formation of epithelial leader cells during wound healing," *Proceedings of the National Academy of Sciences of the United States of America*, vol. 100, pp. 10788 -10793, 2003-09-16 2003.
- [6] M. Poujade, E. Grasland-Mongrain, A. Hertzog, J. Jouanneau, P. Chavrier, B. Ladoux, *et al.*, "Collective migration of an epithelial monolayer in response to a model wound," *Proceedings of the National Academy of Sciences*, vol. 104, pp. 15988-15993, 2007.

- [7] T. Mizoguchi, H. Verkade, J. K. Heath, A. Kuroiwa, and Y. Kikuchi, "Sdf1/Cxcr4 signaling controls the dorsal migration of endodermal cells during zebrafish gastrulation," *Development*, vol. 135, pp. 2521-2529, 2008.
- [8] P. Friedl, J. Locker, E. Sahai, and J. E. Segall, "Classifying collective cancer cell invasion," *Nat Cell Biol*, vol. 14, pp. 777-783, 08//print 2012.
- [9] P. Friedl, "Prespecification and plasticity: shifting mechanisms of cell migration," *Current Opinion in Cell Biology*, vol. 16, pp. 14-23, 2// 2004.
- [10] A. J. Ridley, M. A. Schwartz, K. Burridge, R. A. Firtel, M. H. Ginsberg, G. Borisy, *et al.*, "Cell Migration: Integrating Signals from Front to Back," *Science*, vol. 302, pp. 1704 -1709, 2003-12-05 2003.
- [11] T. E. Angelini, E. Hannezo, X. Trepas, M. Marquez, J. J. Fredberg, and D. A. Weitz, "Glass-like dynamics of collective cell migration," *Proceedings of the National Academy of Sciences*, vol. 108, pp. 4714-4719, 2011.
- [12] J. Zimmermann, M. Basan, and H. Levine, "An instability at the edge of a tissue of collectively migrating cells can lead to finger formation during wound healing," *The European Physical Journal Special Topics*, vol. 223, pp. 1259-1264, 2014/06/01 2014.
- [13] M. Junkin and P. K. Wong, "Probing cell migration in confined environments by plasma lithography," *Biomaterials*, vol. 32, pp. 1848-1855, 2011.

- [14] M. Reffay, M. Parrini, O. Cochet-Escartin, B. Ladoux, A. Buguin, S. Coscoy, *et al.*, "Interplay of RhoA and mechanical forces in collective cell migration driven by leader cells," *Nature cell biology*, vol. 16, pp. 217-223, 2014.
- [15] X. Trepap, M. R. Wasserman, T. E. Angelini, E. Millet, D. A. Weitz, J. P. Butler, *et al.*, "Physical forces during collective cell migration," *Nature physics*, vol. 5, pp. 426-430, 2009.
- [16] D. T. Tambe, C. C. Hardin, T. E. Angelini, K. Rajendran, C. Y. Park, X. Serra-Picamal, *et al.*, "Collective cell guidance by cooperative intercellular forces," *Nature materials*, vol. 10, pp. 469-475, 2011.
- [17] S. Boyden, "The chemotactic effect of mixtures of antibody and antigen on polymorphonuclear leucocytes," *The Journal of experimental medicine*, vol. 115, pp. 453-466, 1962.
- [18] J. Hasan, S. Shnyder, M. Bibby, J. Double, R. Bicknel, and G. Jayson, "Quantitative angiogenesis assays in vivo—a review," *Angiogenesis*, vol. 7, pp. 1-16, 2004.
- [19] S. Chung, R. Sudo, V. Vickerman, I. K. Zervantonakis, and R. D. Kamm, "Microfluidic platforms for studies of angiogenesis, cell migration, and cell-cell interactions. Sixth International Bio-Fluid Mechanics Symposium and Workshop March 28-30, 2008 Pasadena, California," *Ann Biomed Eng*, vol. 38, pp. 1164-77, Mar 2010.

- [20] M. H. Zaki, K. L. Boyd, P. Vogel, M. B. Kastan, M. Lamkanfi, and T. D. Kanneganti, "The NLRP3 inflammasome protects against loss of epithelial integrity and mortality during experimental colitis," *Immunity*, vol. 32, pp. 379-91, Mar 26 2010.
- [21] P. Martin, "Wound healing--aiming for perfect skin regeneration," *Science*, vol. 276, pp. 75-81, Apr 4 1997.
- [22] W. M. Bement, P. Forscher, and M. S. Mooseker, "A Novel Cytoskeletal Structure Involved in Purse String Wound Closure and Cell Polarity Maintenance," *Journal of Cell Biology*, vol. 121, pp. 565-578, May 1993.
- [23] Y. Qian, K. J. Liu, Y. Chen, D. C. Flynn, V. Castranova, and X. Shi, "Cdc42 regulates arsenic-induced NADPH oxidase activation and cell migration through actin filament reorganization," *J Biol Chem*, vol. 280, pp. 3875-84, Feb 4 2005.
- [24] P. Vitorino and T. Meyer, "Modular control of endothelial sheet migration," *Genes & Development*, vol. 22, pp. 3268 -3281, 2008-12-01 2008.
- [25] X. Serra-Picamal, V. Conte, R. Vincent, E. Anon, D. T. Tambe, E. Bazellieres, *et al.*, "Mechanical waves during tissue expansion," *Nature Physics*, 2012.
- [26] S. Raghavan and C. S. Chen, "Micropatterned environments in cell biology," *Advanced Materials*, vol. 16, pp. 1303-1313, 2004.

- [27] S. R. K. Vedula, M. C. Leong, T. L. Lai, P. Hersen, A. J. Kabla, C. T. Lim, *et al.*, "Emerging modes of collective cell migration induced by geometrical constraints," *Proceedings of the National Academy of Sciences of the United States of America*, vol. 109, pp. 12974-12979, 2012.
- [28] C. G. Rolli, H. Nakayama, K. Yamaguchi, J. P. Spatz, R. Kemkemer, and J. Nakanishi, "Switchable adhesive substrates: Revealing geometry dependence in collective cell behavior," *Biomaterials*, vol. 33, pp. 2409-2418, 2012.
- [29] D. L. Nikolić, A. N. Boettiger, D. Bar-Sagi, J. D. Carbeck, and S. Y. Shvartsman, "Role of boundary conditions in an experimental model of epithelial wound healing," *American journal of physiology-cell physiology*, vol. 291, pp. C68-C75, 2006.
- [30] D. J. Cohen, W. J. Nelson, and M. M. Maharbiz, "Galvanotactic control of collective cell migration in epithelial monolayers," *Nature materials*, 2014.
- [31] C. R. Keese, J. Wegener, S. R. Walker, and I. Giaever, "Electrical wound-healing assay for cells in vitro," *Proceedings of the National Academy of Sciences of the United States of America*, vol. 101, pp. 1554-1559, 2004.
- [32] D. T. Tambe, U. Croutelle, X. Trepate, C. Y. Park, J. H. Kim, E. Millet, *et al.*, "Monolayer Stress Microscopy: Limitations, Artifacts, and Accuracy of Recovered Intercellular Stresses," *PLoS ONE*, vol. 8, p. e55172, 2013.
- [33] Y. Yang and P. K. Wong, "A Plasma Lithography Microengineered Assay for Studying Architecture Dependent Wound Healing of Endothelial Cells," in

The 15th International Conference on Miniaturized Systems for Chemistry and Life Sciences, 2011, pp. 326-328.

- [34] J. V. Cordeiro and A. Jacinto, "The role of transcription-independent damage signals in the initiation of epithelial wound healing," *Nature Reviews Molecular Cell Biology*, vol. 14, pp. 249-262, 2013.
- [35] A. J. Kabla, "Collective cell migration: leadership, invasion and segregation," *Journal of The Royal Society Interface*, vol. 9, pp. 3268-3278, 2012.
- [36] H. Gerhardt, M. Golding, M. Fruttiger, C. Ruhrberg, A. Lundkvist, A. Abramsson, *et al.*, "VEGF guides angiogenic sprouting utilizing endothelial tip cell filopodia," *The Journal of cell biology*, vol. 161, pp. 1163-1177, 2003.
- [37] R. Farooqui and G. Fenteany, "Multiple rows of cells behind an epithelial wound edge extend cryptic lamellipodia to collectively drive cell-sheet movement," *Journal of Cell Science*, vol. 118, pp. 51-63, January 1, 2005 2005.
- [38] M. T. Janet, G. Cheng, J. A. Tyrrell, S. A. Wilcox-Adelman, Y. Boucher, R. K. Jain, *et al.*, "Mechanical compression drives cancer cells toward invasive phenotype," *Proceedings of the National Academy of Sciences of the United States of America*, vol. 109, pp. 911-916, 2012.
- [39] P. Vitorino, M. Hammer, J. Kim, and T. Meyer, "A steering model of endothelial sheet migration recapitulates monolayer integrity and directed collective migration," *Mol Cell Biol*, vol. 31, pp. 342-50, Jan 2011.

- [40] D. K. Nordstrom, "Worldwide Occurrences of Arsenic in Ground Water," *Science*, vol. 296, pp. 2143-2145, June 21, 2002 2002.
- [41] B. K. Mandal and K. T. Suzuki, "Arsenic round the world: a review," *Talanta*, vol. 58, pp. 201-235, 2002.
- [42] WHO, "Guidelines for Drinking-water Quality," Geneva2008.
- [43] K. Jomova, Z. Jenisova, M. Feszterova, S. Baros, J. Liska, D. Hudecova, *et al.*, "Arsenic: toxicity, oxidative stress and human disease," *Journal of Applied Toxicology*, vol. 31, pp. 95-107, 2011.
- [44] A. Lencinas, D. M. Broka, J. H. Konieczka, S. E. Klewer, P. B. Antin, T. D. Camenisch, *et al.*, "Arsenic Exposure Perturbs Epithelial-Mesenchymal Cell Transition and Gene Expression In a Collagen Gel Assay," *Toxicological Sciences*, vol. 116, pp. 273-285, July 1, 2010 2010.
- [45] S. L. Yancy, E. A. Shelden, R. R. Gilmont, and M. J. Welsh, "Sodium arsenite exposure alters cell migration, focal adhesion localization and decreases tyrosine phosphorylation of focal adhesion kinase in H9C2 myoblasts," *Toxicol Sci*, vol. 84, pp. 278-86, Apr 2005.
- [46] X. Cai, Y. Shen, Q. Zhu, P. Jia, Y. Yu, L. Zhou, *et al.*, "Arsenic trioxide-induced apoptosis and differentiation are associated respectively with mitochondrial transmembrane potential collapse and retinoic acid signaling pathways in acute promyelocytic leukemia," *Leukemia*, vol. 14, pp. 262-270, 2000.

- [47] H. Jintian, "The effect of Arsenite on properties of keratinocytes cell culture," Master, National Cheng Kung University, Taiwan, 2004.
- [48] K. Souza, D. A. Maddock, Q. Zhang, J. Chen, C. Chiu, S. Mehta, *et al.*, "Arsenite activation of P13K/AKT cell survival pathway is mediated by p38 in cultured human keratinocytes," *Molecular medicine (Cambridge, Mass.)*, vol. 7, pp. 767-772, 11/ 2001.
- [49] R. J. Cain and A. J. Ridley, "Phosphoinositide 3-kinases in cell migration," *Biology of the Cell*, vol. 101, pp. 13-29, 2009.
- [50] M. Bessho, T. Aki, T. Funakoshi, K. Unuma, K. Noritake, C. Kato, *et al.*, "Rho-Kinase Inhibitor Y-27632 Attenuates Arsenic Trioxide Toxicity in H9c2 Cardiomyoblastoma Cells," *Cardiovascular Toxicology*, vol. 13, pp. 267-277, 2013/09/01 2013.
- [51] A. C. Porter, G. R. Fanger, and R. R. Vaillancourt, "Signal transduction pathways regulated by arsenate and arsenite," *Oncogene*, vol. 18, pp. 7794-802, Dec 16 1999.
- [52] C. Huang, K. Jacobson, and M. D. Schaller, "MAP kinases and cell migration," *J Cell Sci*, vol. 117, pp. 4619-28, Sep 15 2004.
- [53] A. Lau, S. A. Whitman, M. C. Jaramillo, and D. D. Zhang, "Arsenic-mediated activation of the Nrf2-Keap1 antioxidant pathway," *J Biochem Mol Toxicol*, vol. 27, pp. 99-105, Feb 2013.

- [54] R. Hayashi, N. Himori, K. Taguchi, Y. Ishikawa, K. Uesugi, M. Ito, *et al.*, "The Role of Nrf2-Mediated Defense System in Corneal Epithelial Wound Healing," *Free Radical Biology and Medicine*, 2013.
- [55] R. Riahi, M. Long, Y. Yang, Z. Dean, D. D. Zhang, M. J. Slepian, *et al.*, "Single cell gene expression analysis in injury-induced collective cell migration," *Integrative Biology*, vol. 6, pp. 192-202, 2014.
- [56] K. Wolf and P. Friedl, "Molecular mechanisms of cancer cell invasion and plasticity," *British Journal of Dermatology*, vol. 154, pp. 11-15, 2006.
- [57] W.-P. Tseng, "Effects and dose-response relationships of skin cancer and blackfoot disease with arsenic," *Environmental health perspectives*, vol. 19, p. 109, 1977.
- [58] R. Chowdhury, R. Chatterjee, A. K. Giri, C. Mandal, and K. Chaudhuri, "Arsenic-induced cell proliferation is associated with enhanced ROS generation, Erk signaling and CyclinA expression," *Toxicology Letters*, vol. 198, pp. 263-271, 10/5/ 2010.
- [59] H. Pan, H. Wang, L. Zhu, L. Mao, L. Qiao, and X. Su, "The role of Nrf2 in migration and invasion of human glioma cell U251," *World neurosurgery*, vol. 80, pp. 363-370, 2013.
- [60] G. Rachakonda, K. R. Sekhar, D. Jowhar, P. C. Samson, J. P. Wikswo, R. D. Beauchamp, *et al.*, "Increased cell migration and plasticity in Nrf2-deficient cancer cell lines," *Oncogene*, vol. 29, pp. 3703-3714, 2010.

- [61] T. Ashino, M. Yamamoto, T. Yoshida, and S. Numazawa, "Redox-Sensitive Transcription Factor Nrf2 Regulates Vascular Smooth Muscle Cell Migration and Neointimal Hyperplasia," *Arteriosclerosis, Thrombosis, and Vascular Biology*, vol. 33, pp. 760-768, April 1, 2013 2013.
- [62] D. Kelly and P. J. Prendergast, "Mechano-regulation of stem cell differentiation and tissue regeneration in osteochondral defects," *Journal of biomechanics*, vol. 38, pp. 1413-1422, 2005.
- [63] H. C. Chen, "Boyden chamber assay," *Methods Mol Biol*, vol. 294, pp. 15-22, 2005.
- [64] L. Rodriguez, X. Wu, and J.-L. Guan, "Wound-Healing Assay," in *Cell Migration*. vol. 294, J.-L. Guan, Ed., ed: Humana Press, 2005, pp. 23-29.
- [65] J. Hasan, S. D. Shnyder, M. Bibby, J. A. Double, R. Bicknel, and G. C. Jayson, "Quantitative angiogenesis assays in vivo--a review," *Angiogenesis*, vol. 7, pp. 1-16, 2004.
- [66] R. Riahi, Y. Yang, D. D. Zhang, and P. K. Wong, "Advances in Wound-Healing Assays for Probing Collective Cell Migration," *Journal of Laboratory Automation*, vol. 17, pp. 59-65, 2012.
- [67] P. Y. Yue, E. P. Leung, N. Mak, and R. N. Wong, "A simplified method for quantifying cell migration/wound healing in 96-well plates," *Journal of biomolecular screening*, vol. 15, pp. 427-433, 2010.

- [68] K. J. Simpson, L. M. Selfors, J. Bui, A. Reynolds, D. Leake, A. Khvorova, *et al.*, "Identification of genes that regulate epithelial cell migration using an siRNA screening approach," *Nature cell biology*, vol. 10, pp. 1027-1038, 2008.
- [69] E. Fong, S. Tzllil, and D. A. Tirrell, "Boundary crossing in epithelial wound healing," *Proceedings of the National Academy of Sciences*, vol. 107, pp. 19302-19307, 2010.
- [70] J. Lee, Y.-L. Wang, F. Ren, and T. P. Lele, "Stamp Wound Assay for Studying Coupled Cell Migration and Cell Debris Clearance," *Langmuir*, vol. 26, pp. 16672-16676, 2010.
- [71] B. Pratt, A. Harris, J. Morrow, and J. Madri, "Mechanisms of cytoskeletal regulation. Modulation of aortic endothelial cell spectrin by the extracellular matrix," *The American journal of pathology*, vol. 117, p. 349, 1984.
- [72] E. G. Fischer, A. Stingl, and C. James Kirkpatrick, "Migration assay for endothelial cells in multiwells: Applications to studies on the effect of opioids," *Journal of immunological methods*, vol. 128, pp. 235-239, 1990.
- [73] C. Legrand, C. Gilles, J.-M. Zahm, M. Polette, A.-C. Buisson, H. Kaplan, *et al.*, "Airway Epithelial Cell Migration Dynamics: MMP-9 Role in Cell–Extracellular Matrix Remodeling," *The Journal of Cell Biology*, vol. 146, pp. 517-529, July 26, 1999 1999.

- [74] C. G. Conant, J. T. Nevill, M. Schwartz, and C. Ionescu-Zanetti, "Wound Healing Assays in Well Plate—Coupled Microfluidic Devices with Controlled Parallel Flow," *Journal of the Association for Laboratory Automation*, vol. 15, pp. 52-57, 2010.
- [75] E. Noiri, Y. Hu, W. F. Bahou, C. R. Keese, I. Giaever, and M. S. Goligorsky, "Permissive role of nitric oxide in endothelin-induced migration of endothelial cells," *Journal of Biological Chemistry*, vol. 272, pp. 1747-1752, 1997.
- [76] M. R. Koller, E. G. Hanania, J. Stevens, T. M. Eisfeld, G. C. Sasaki, A. Fieck, *et al.*, "High-throughput laser-mediated in situ cell purification with high purity and yield," *Cytometry Part A*, vol. 61, pp. 153-161, 2004.
- [77] M. D. Zordan, C. P. Mill, D. J. Riese, and J. F. Leary, "A high throughput, interactive imaging, bright-field wound healing assay," *Cytometry Part A*, vol. 79, pp. 227-232, 2011.
- [78] C. M. Nelson, R. P. Jean, J. L. Tan, W. F. Liu, N. J. Sniadecki, A. A. Spector, *et al.*, "Emergent patterns of growth controlled by multicellular form and mechanics," *Proceedings of the National Academy of Sciences of the United States of America*, vol. 102, pp. 11594-11599, 2005.
- [79] S. R. K. Vedula, M. C. Leong, T. L. Lai, P. Hersen, A. J. Kabla, C. T. Lim, *et al.*, "Emerging modes of collective cell migration induced by geometrical constraints," *Proceedings of the National Academy of Sciences*, vol. 109, pp. 12974-12979, 2012.

- [80] C. M. Nelson, R. P. Jean, J. L. Tan, W. F. Liu, N. J. Sniadecki, A. A. Spector, *et al.*, "Emergent patterns of growth controlled by multicellular form and mechanics," *Proceedings of the National Academy of Sciences of the United States of America*, vol. 102, pp. 11594 -11599, 2005-08-16 2005.
- [81] M. Dembo and Y.-L. Wang, "Stresses at the Cell-to-Substrate Interface during Locomotion of Fibroblasts," *Biophysical Journal*, vol. 76, pp. 2307-2316, 4// 1999.
- [82] J. Fu, Y.-K. Wang, M. T. Yang, R. A. Desai, X. Yu, Z. Liu, *et al.*, "Mechanical regulation of cell function with geometrically modulated elastomeric substrates," *Nature methods*, vol. 7, pp. 733-736, 2010.
- [83] R. J. Adrian and J. Westerweel, *Particle image velocimetry*: Cambridge University Press, 2011.
- [84] X. Trepap, C. T. Lim, and B. Ladoux, "Epithelial bridges maintain tissue integrity during collective cell migration."
- [85] M. Junkin, J. Watson, J. P. V. Geest, and P. K. Wong, "Template-Guided Self-Assembly of Colloidal Quantum Dots Using Plasma Lithography," *Advanced Materials*, vol. 21, pp. 1247-1251, 2009.
- [86] M. Junkin, S. L. Leung, Y. Yang, Y. Lu, J. Volmering, and P. K. Wong, "Plasma lithography surface patterning for creation of cell networks," *Journal of visualized experiments: JoVE*, 2011.

- [87] Y. Yang, J. Volmering, M. Junkin, and P. K. Wong, "Comparative assembly of colloidal quantum dots on surface templates patterned by plasma lithography," *Soft Matter*, vol. 7, pp. 10085-10090, 2011.
- [88] J. Keyes, M. Junkin, J. Cappello, X. Wu, and P. K. Wong, "Evaporation-induced assembly of biomimetic polypeptides," *Applied Physics Letters*, vol. 93, p. 023120, 2008.
- [89] D. H. Ausprunk and J. Folkman, "Migration and proliferation of endothelial cells in preformed and newly formed blood vessels during tumor angiogenesis," *Microvascular research*, vol. 14, pp. 53-65, 1977.
- [90] W. M. Bement, P. Forscher, and M. S. Mooseker, "A novel cytoskeletal structure involved in purse string wound closure and cell polarity maintenance," *The Journal of cell biology*, vol. 121, pp. 565-578, 1993.
- [91] S. Rausch, T. Das, J. R. Soin é T. W. Hofmann, C. H. Boehm, U. S. Schwarz, *et al.*, "Polarizing cytoskeletal tension to induce leader cell formation during collective cell migration," *Biointerphases*, vol. 8, p. 32, 2013.
- [92] L. Liu, G. Duclos, B. Sun, J. Lee, A. Wu, Y. Kam, *et al.*, "Minimization of thermodynamic costs in cancer cell invasion," *Proceedings of the National Academy of Sciences*, vol. 110, pp. 1686-1691, 2013.
- [93] K. J. Cheung, E. Gabrielson, Z. Werb, and A. J. Ewald, "Collective invasion in breast cancer requires a conserved basal epithelial program," *Cell*, vol. 155, pp. 1639-1651, 2013.

- [94] A. A. Khalil and P. Friedl, "Determinants of leader cells in collective cell migration," *Integrative Biology*, vol. 2, pp. 568-574, 2010.
- [95] A. J. Ridley, M. A. Schwartz, K. Burridge, R. A. Firtel, M. H. Ginsberg, G. Borisy, *et al.*, "Cell migration: integrating signals from front to back," *Science*, vol. 302, pp. 1704-1709, 2003.
- [96] N. Q. Balaban, U. S. Schwarz, D. Riveline, P. Goichberg, G. Tzur, I. Sabanay, *et al.*, "Force and focal adhesion assembly: a close relationship studied using elastic micropatterned substrates," *Nature cell biology*, vol. 3, pp. 466-472, 2001.
- [97] A. Munjal and T. Lecuit, "Actomyosin networks and tissue morphogenesis," *Development*, vol. 141, pp. 1789-1793, May 2014.
- [98] S. Huveneers, J. Oldenburg, E. Spanjaard, G. van der Krogt, I. Grigoriev, A. Akhmanova, *et al.*, "Vinculin associates with endothelial VE-cadherin junctions to control force-dependent remodeling," *The Journal of Cell Biology*, vol. 196, pp. 641-652, March 5, 2012 2012.
- [99] J. Millan, R. Cain, N. Reglero-Real, C. Bigarella, B. Marcos-Ramiro, L. Fernandez-Martin, *et al.*, "Adherens junctions connect stress fibres between adjacent endothelial cells," *BMC Biology*, vol. 8, p. 11, 2010.
- [100] S. Huveneers, J. Oldenburg, E. Spanjaard, G. van der Krogt, I. Grigoriev, A. Akhmanova, *et al.*, "Vinculin associates with endothelial VE-cadherin

- junctions to control force-dependent remodeling," *J Cell Biol*, vol. 196, pp. 641-52, Mar 5 2012.
- [101] O. Ilina and P. Friedl, "Mechanisms of collective cell migration at a glance," *Journal of cell science*, vol. 122, pp. 3203-3208, 2009.
- [102] R. B. VAUGHAN and J. P. TRINKAUS, "Movements of Epithelial Cell Sheets In Vitro," *Journal of Cell Science*, vol. 1, pp. 407-413, December 1, 1966 1966.
- [103] N. Gjorevski and C. M. Nelson, "Endogenous patterns of mechanical stress are required for branching morphogenesis," *Integrative Biology*, vol. 2, pp. 424-434, 2010.
- [104] N. C. Rivron, E. J. Vrij, J. Rouwkema, S. Le Gac, A. van den Berg, R. K. Truckenmüller, *et al.*, "Tissue deformation spatially modulates VEGF signaling and angiogenesis," *Proceedings of the National Academy of Sciences*, vol. 109, pp. 6886-6891, 2012.
- [105] A. Shay-Salit, M. Shushy, E. Wolfovitz, H. Yahav, F. Breviario, E. Dejana, *et al.*, "VEGF receptor 2 and the adherens junction as a mechanical transducer in vascular endothelial cells," *Proceedings of the National Academy of Sciences*, vol. 99, pp. 9462-9467, 2002.
- [106] K. Burridge and E. S. Wittchen, "The tension mounts: stress fibers as force-generating mechanotransducers," *The Journal of cell biology*, vol. 200, pp. 9-19, 2013.

- [107] D. Franco, F. Milde, M. Klingauf, F. Orsenigo, E. Dejana, D. Poulikakos, *et al.*, "Accelerated endothelial wound healing on microstructured substrates under flow," *Biomaterials*, vol. 34, pp. 1488-1497, 2// 2013.
- [108] M. Murrell, R. Kamm, and P. Matsudaira, "Tension, free space, and cell damage in a microfluidic wound healing assay," *PloS one*, vol. 6, p. e24283, 2011.
- [109] C. M. Nelson, "Geometric control of tissue morphogenesis," *Biochimica et Biophysica Acta (BBA)-Molecular Cell Research*, vol. 1793, pp. 903-910, 2009.
- [110] S. A. Ruiz and C. S. Chen, "Emergence of patterned stem cell differentiation within multicellular structures," *Stem cells*, vol. 26, pp. 2921-2927, 2008.
- [111] K. Doxzen, S. R. K. Vedula, M. C. Leong, H. Hirata, N. S. Gov, A. J. Kabla, *et al.*, "Guidance of collective cell migration by substrate geometry," *Integrative Biology*, vol. 5, pp. 1026-1035, 2013.
- [112] A. RA, "[not available]," *REV ARGENT DERM*, vol. 22, p. 461, 1938.
- [113] W. P. Tseng, H. M. Chu, S. W. How, J. M. Fong, C. S. Lin, and S. Yeh, "PREVALENCE OF SKIN CANCER IN AN ENDEMIC AREA OF CHRONIC ARSENICISM IN TAIWAN," *Journal of the National Cancer Institute*, vol. 40, pp. 453-&, 1968.
- [114] U. Schuhmacher-Wolz, H. H. Dieter, D. Klein, and K. Schneider, "Oral exposure to inorganic arsenic: evaluation of its carcinogenic and non-

- carcinogenic effects," *Critical Reviews in Toxicology*, vol. 39, pp. 271-298, 2009.
- [115] L. C. Platanias, "Biological Responses to Arsenic Compounds," *Journal of Biological Chemistry*, vol. 284, pp. 18583-18587, July 10, 2009 2009.
- [116] S. X. Liu, M. Athar, I. Lippai, C. Waldren, and T. K. Hei, "Induction of oxyradicals by arsenic: Implication for mechanism of genotoxicity," *Proceedings of the National Academy of Sciences*, vol. 98, pp. 1643-1648, February 13, 2001 2001.
- [117] D. Sinha, J. Biswas, and A. Bishayee, "Nrf2-mediated redox signaling in arsenic carcinogenesis: a review," *Archives of Toxicology*, vol. 87, pp. 383-396, 2013/02/01 2013.
- [118] J. Pi, W. Qu, J. M. Reece, Y. Kumagai, and M. P. Waalkes, "Transcription factor Nrf2 activation by inorganic arsenic in cultured keratinocytes: involvement of hydrogen peroxide," *Experimental Cell Research*, vol. 290, pp. 234-245, 2003.
- [119] A. Lau, S. A. Whitman, M. C. Jaramillo, D. D. Zhang, D. Sinha, J. Biswas, *et al.*, "Arsenic-Mediated Activation of the Nrf2-Keap1 Antioxidant Pathway Nrf2-mediated redox signaling in arsenic carcinogenesis: a review," *Journal of Biochemical and Molecular Toxicology*, vol. 27, pp. 99-105, 2013-02-01 2013.

- [120] R. Hayashi, N. Himori, K. Taguchi, Y. Ishikawa, K. Uesugi, M. Ito, *et al.*,
"The role of the Nrf2-mediated defense system in corneal epithelial wound
healing," *Free Radical Biology and Medicine*, vol. 61, pp. 333-342, 2013.
- [121] R. Riahi, M. Long, Y. Yang, Z. Dean, D. D. Zhang, M. J. Slepian, *et al.*,
"Single cell gene expression analysis in injury-induced collective cell
migration," *Integrative Biology*, 2014.
- [122] P. Vitorino and T. Meyer, "Modular control of endothelial sheet migration,"
Genes Dev, vol. 22, pp. 3268-81, Dec 1 2008.
- [123] T. Omelchenko, J. M. Vasiliev, I. M. Gelfand, H. H. Feder, and E. M. Bonder,
"Rho-dependent formation of epithelial "leader" cells during wound healing,"
Proc Natl Acad Sci U S A, vol. 100, pp. 10788-93, Sep 16 2003.
- [124] M. Poujade, E. Grasland-Mongrain, A. Hertzog, J. Jouanneau, P. Chavrier, B.
Ladoux, *et al.*, "Collective migration of an epithelial monolayer in response to
a model wound," *Proc Natl Acad Sci U S A*, vol. 104, pp. 15988-93, Oct 9
2007.
- [125] J. M. Tse, G. Cheng, J. A. Tyrrell, S. A. Wilcox-Adelman, Y. Boucher, R. K.
Jain, *et al.*, "Mechanical compression drives cancer cells toward invasive
phenotype," *Proc Natl Acad Sci U S A*, vol. 109, pp. 911-6, Jan 17 2012.
- [126] P. Rosen and D. S. Misfeldt, "Cell density determines epithelial migration in
culture," *Proceedings of the National Academy of Sciences*, vol. 77, pp. 4760-
4763, 1980.

- [127] K. Burton and D. L. Taylor, "Traction forces of cytokinesis measured with optically modified elastic substrata," *Nature*, vol. 385, pp. 450-454, 1997.
- [128] R. Nickson, J. McArthur, W. Burgess, K. M. Ahmed, P. Ravenscroft, and M. Rahman, "Arsenic poisoning of Bangladesh groundwater," *Nature*, vol. 395, pp. 338-338, 1998.